

# Fast Construction of Partitioned Learned Bloom Filter with Theoretical Guarantees

Atsuki Sato

Yusuke Matsui

*Department of Information and Communication Engineering*

*Graduate School of Information Science and Technology*

*The University of Tokyo, Japan*

A\_SATO@HAL.T.U-TOKYO.AC.JP

MATSUI@HAL.T.U-TOKYO.AC.JP

## Abstract

Bloom filter is a widely used classic data structure for approximate membership queries. Learned Bloom filters improve memory efficiency by leveraging machine learning, with the partitioned learned Bloom filter (PLBF) being among the most memory-efficient variants. However, PLBF suffers from high computational complexity during construction, specifically  $\mathcal{O}(N^3k)$ , where  $N$  and  $k$  are hyperparameters. In this paper, we propose three methods—fast PLBF, fast PLBF++, and fast PLBF#—that reduce the construction complexity to  $\mathcal{O}(N^2k)$ ,  $\mathcal{O}(Nk \log N)$ , and  $\mathcal{O}(Nk \log k)$ , respectively. Fast PLBF preserves the original PLBF structure and memory efficiency. Although fast PLBF++ and fast PLBF# may have different structures, we theoretically prove they are equivalent to PLBF under ideal data distribution. Furthermore, we theoretically bound the difference in memory efficiency between PLBF and fast PLBF++ for non-ideal scenarios. Experiments on real-world datasets demonstrate that fast PLBF, fast PLBF++, and fast PLBF# are up to 233, 761, and 778 times faster to construct than original PLBF, respectively. Additionally, fast PLBF maintains the same data structure as PLBF, and fast PLBF++ and fast PLBF# achieve nearly identical memory efficiency.

**Keywords:** learned Bloom filter, learned index, membership query, optimization, dynamic programming

## 1 Introduction

Bloom filter is a memory-efficient probabilistic data structure for approximate membership queries. While Bloom filters produce false positives due to hash collisions, they do not produce false negatives. Because of this favorable property, they are widely used in various memory-constrained applications such as networks, databases, etc. There is a trade-off between the size of the Bloom filter and the false positive rate (FPR); the lower the FPR, the larger the filter needed. According to Pagh et al. (2005), a data structure that stores a set of  $n$  elements with an FPR of  $F$  needs at least  $n \log_2(1/F)$  bits of memory. However, in practical applications, the data set and/or query has a certain structure, and thus we may be able to achieve better efficiency than this theoretical limit. Innovatively, Kraska et al. (2018) integrate a machine learning model with a Bloom filter and use this model as a prefilter, further reducing the space requirement. Such a Bloom filter is called a learned Bloom filter (LBF) and has been actively studied. In particular, partitioned learned Bloom filter (PLBF) (Vaidya et al., 2021) solves an optimization problem using dynamic programming

Method	Construction Time	Memory-Efficiency Comparison with PLBF
PLBF	$\mathcal{O}(N^3k)$	-
Fast PLBF	$\mathcal{O}(N^2k)$	Always identical
Fast PLBF++	$\mathcal{O}(Nk \log N + Nk^2)$ $\rightarrow \mathcal{O}(Nk \log N)$	Identical under ideal conditions + Theoretical bound under non-ideal conditions
Fast PLBF#	$\mathcal{O}(Nk \log k)$	Identical under ideal conditions

Table 1: Comparison of PLBF (Vaidya et al., 2021) and our proposed methods. The second and third rows show the results of our previously published conference paper (Sato and Matsui, 2023). The fourth and fifth rows show the new contributions made in this paper.

to find the optimal configuration of the prefilter and the backup filters, which allows almost full utilization of the machine learning performance.

However, PLBF requires a lot of time for its construction. This is because  $\mathcal{O}(N^3k)$  of computation is required to solve the optimization problem, where  $N$  and  $k$  are hyperparameters of PLBF. As  $N$  and  $k$  increase, the PLBF becomes more memory-efficient but the construction time becomes unrealistically long.

We propose three methods to speed up the construction of PLBF while maintaining their excellent memory efficiency: fast PLBF, fast PLBF++, and fast PLBF#. The computational complexity for solving the optimization problem of fast PLBF, fast PLBF++, and fast PLBF# is  $\mathcal{O}(N^2k)$ ,  $\mathcal{O}(Nk \log N)$ , and  $\mathcal{O}(Nk \log k)$ , respectively. Fast PLBF has the same data structure as PLBF, that is, it achieves the same memory efficiency as PLBF. Although fast PLBF++ and fast PLBF# do not necessarily have the same data structure as PLBF, we theoretically guarantee that they have the same data structures as PLBF under an intuitive and ideal condition on the distribution. Furthermore, we theoretically bound the difference of memory efficiency between (fast) PLBF and fast PLBF++/#.

We evaluate our methods using real-world data sets and artificial data sets. The results show that (i) fast PLBF, fast PLBF++, and fast PLBF# can be constructed at most 233, 761, and 778 times faster than PLBF, (ii) fast PLBF achieves exactly the same memory efficiency as PLBF, and (iii) fast PLBF++ and fast PLBF# achieve almost the same memory efficiency as PLBF, and the difference is within limits guaranteed by our theorem.

This study builds on a previous shorter conference paper (Sato and Matsui, 2023). We significantly extend this work and make several further contributions, as summarized in Table 1. First, we have improved the worst-case computational complexity of fast PLBF++ from  $\mathcal{O}(Nk \log N + Nk^2)$  to  $\mathcal{O}(Nk \log N)$  by carefully observing the optimization problem and modifying parts of the algorithm. Second, we have extended the theoretical guarantee of the memory efficiency of fast PLBF++. Previously, memory efficiency was only guaranteed under ideal circumstances. However, it is now guaranteed even under non-ideal conditions. Third, we have proposed and given a theoretical guarantee for fast PLBF#, which has an even smaller computational complexity than fast PLBF++. Furthermore, we have confirmed that the theoretical guarantee fits well with the experimental results.

The remainder of this paper is organized as follows. In Section 2, we present the related work. In Section 3, we give preliminaries consisting of two parts. First, we describe PLBF, including its architecture, the optimization problem it addresses, and its solution. Next, we introduce the *matrix problem* and the related algorithms used in the core of our acceleration. In Section 4, we propose our three methods for fast PLBF construction. In Section 4.1, we propose fast PLBF and give a proof that it has exactly the same memory efficiency as PLBF. In Section 4.2 and Section 4.3, we propose fast PLBF++ and fast PLBF#, respectively, and give theoretical guarantees for the difference in memory efficiency between them and PLBF. In Section 5, we present extensive experiments that demonstrate these methods’ effectiveness and our theorems’ validity.

## 2 Related Work

Our work is in the context of LBF, which uses machine learning to improve the performance of the Bloom filter. We first introduce the Bloom filter and its variants in Section 2.1, and then present related work on LBF in Section 2.2.

### 2.1 Bloom Filter and Its Variants

The Bloom filter (Bloom, 1970) is a traditional data structure that answers approximate membership queries. An approximate membership query is a query that determines whether a set  $\mathcal{S}$  contains an element  $q$ , while allowing false positives with some probability. Bloom filters are often used in contexts such as networks (Broder and Mitzenmacher, 2004; Tarkoma et al., 2011; Geravand and Ahmadi, 2013) and databases (Chang et al., 2008; Goodrich and Mitzenmacher, 2011; Lu et al., 2012), where memory constraints are tight and a small rate of false positives is tolerable.

The Bloom filter is a data structure consisting of an  $m$ -bit bit array,  $\mathbf{b}$ , and  $k$  independent hash functions,  $h_1, h_2, \dots, h_k$ , each of which maps an input to an integer value between 1 and  $m$ . To set up a Bloom filter, all bits of  $\mathbf{b}$  are initially set to 0, and then for each element  $x$  ( $\in \mathcal{S}$ ) and for each  $i$  ( $\in \{1, 2, \dots, k\}$ ), set the bit  $b_{h_i(x)}$  to 1. To check whether an element  $q$  is in the set  $\mathcal{S}$ , the Bloom filter checks the bits at positions  $h_1(q), h_2(q), \dots, h_k(q)$  in the bit array  $\mathbf{b}$ . If any of these bits is 0, then  $q$  is definitely not in the set  $\mathcal{S}$  (no false negatives occur). If all of these bits are 1, the Bloom filter indicates that  $q$  is in the set  $\mathcal{S}$ . However, due to the possibility of hash collisions, this may not be correct, leading to a false positive. The number of bits the Bloom filter requires to achieve an FPR of  $F$  ( $\in (0, 1)$ ) is

$$(\log_2 e) \cdot |\mathcal{S}| \log_2 \frac{1}{F}. \quad (1)$$

It is known that the lower bound for the number of bits required for a given FPR of  $F$  is  $|\mathcal{S}| \log_2 (1/F)$ , so this means that a Bloom filter uses  $\log_2 e \approx 1.44$  times the number of bits of the theoretical lower bound.

Several variants of Bloom filters have been proposed. One of the most representative variants is the Cuckoo filter (Fan et al., 2014). The Cuckoo filter is more memory-efficient than the original Bloom filter and supports dynamic addition and removal of elements. In addition, various derivatives such as Vacuum filter (Wang and Zhou, 2019), Xor filter (Graf and Lemire, 2020), and Ribbon filter (Dillinger and Walzer, 2021) have been proposed with

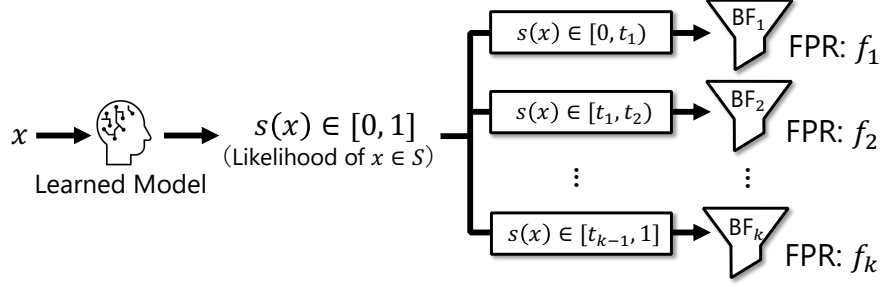


Figure 1: PLBF partitions the score space into  $k$  regions and assigns backup Bloom filters with different FPRs to each region.

the aim of achieving memory efficiency close to the theoretical lower bound and high query speeds. A variant of the Bloom filter with this lower bound has also been proposed (Pagh et al., 2005), but it is so complex that it is difficult to implement in practice.

## 2.2 Learned Bloom Filter

Bloom filter and B-tree (and their variants) are commonly employed as indexing structures in database systems. Kraska et al. (2018) showed that combining these index data structures with machine learning models has the potential to achieve memory savings, and they named these new index data structures “learned indexes.” The main idea behind the learned index is based on the following two points: (i) classical index data structures are essentially “models” that make some kind of prediction, and (ii) machine learning models have the potential to exploit the structural properties of data and queries more efficiently than conventional index data structures. In fact, Kraska et al. showed that by replacing B-trees with machine learning models, it is possible to achieve query response speeds 1.5 to 3 times faster than B-trees while saving nearly 100 times less memory experimentally. This plain learning-augmented B-tree did not support insertion or deletion, and was limited to the case of an one-dimensional array. However, inspired by the research of Kraska et al., various proposals have been made, including those that support insertion and deletion (Ferragina and Vinciguerra, 2020; Ding et al., 2020; Dai et al., 2020; Zhang et al., 2022) and those that extend to multi-dimensional cases (Nathan et al., 2020; Ding et al., 2020; Li et al., 2020; Gu et al., 2023). In addition, there is a lot of research that integrates machine learning with other data structures, such as count-min sketches (Hsu et al., 2019; Zhang et al., 2020) and binary search trees (Lin et al., 2022).

LBF is a type of learned index that extends a Bloom filter with machine learning. The original LBF proposed by Kraska et al. (2018) consists of a single machine learning model and a single backup Bloom filter. The machine learning model is trained to solve the binary classification task of determining whether an input element is in the set  $\mathcal{S}$  or not. This training is done using the set  $\mathcal{S}$  and the set  $\mathcal{Q}$ , where  $\mathcal{Q}$  consists of elements that are not in the set  $\mathcal{S}$ . In many real-world applications,  $\mathcal{Q}$  can be obtained from past queries that are not in  $\mathcal{S}$ . When this LBF responds to a query, if the machine learning model predicts

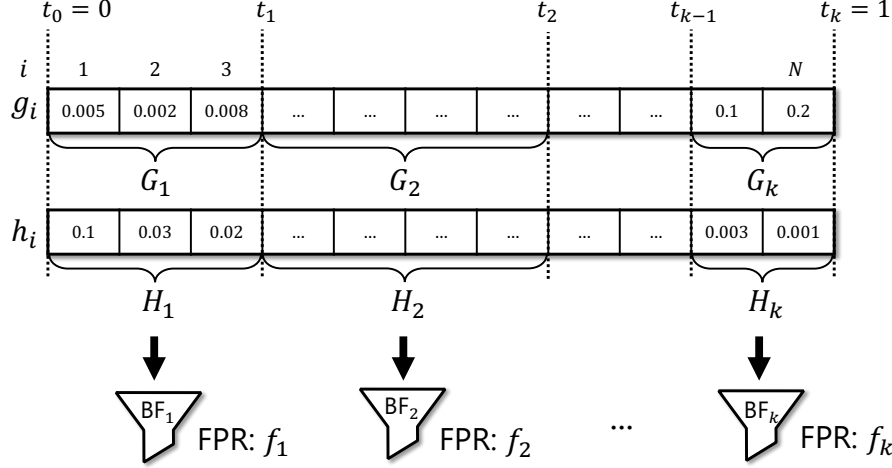


Figure 2: PLBF divides the score space into  $N$  segments and then clusters the  $N$  segments into  $k$  regions. PLBF uses dynamic programming to find the optimal way to cluster segments into regions.

that the query is contained in the set, the LBF immediately responds that the query is contained in the set. Otherwise, the backup Bloom filter is consulted, and its result is used as the final answer. By using this hybrid approach, the LBF retains the important property of Bloom filters of having no false negatives, while taking advantage of the machine learning model’s ability to efficiently capture the structure of  $\mathcal{S}$  and  $\mathcal{Q}$ .

### 3 Preliminaries

This chapter gives the preliminaries. First, we give a detailed explanation of PLBF, one of the state-of-the-art LBFs (Section 3.1). Next, we introduce the *matrix problem* and the classes of matrices related to the problem (Section 3.2).

#### 3.1 Partitioned Learned Bloom Filter

First, we define terms to describe PLBF (Vaidya et al., 2021) and explain its design. Let  $\mathcal{S}$  be a set of elements for which the Bloom filter is to be built, and let  $\mathcal{Q}$  be the set of elements not included in  $\mathcal{S}$  that is used when constructing PLBF ( $\mathcal{S} \cap \mathcal{Q} = \emptyset$ ). The elements included in  $\mathcal{S}$  are called keys, and those not included are called non-keys.  $\mathcal{Q}$  is employed to approximate the distribution of non-key queries. To build PLBF, a machine learning model is trained to predict whether a given element  $x$  is included in the set  $\mathcal{S}$  or  $\mathcal{Q}$ . For a given element  $x$ , the machine learning model outputs a score  $s(x)$  ( $\in [0, 1]$ ). The score  $s(x)$  indicates “how likely is  $x$  to be included in the set  $\mathcal{S}$ .” PLBF partitions the score space  $[0, 1]$  into  $k$  regions and assigns backup Bloom filters with different FPRs to each region (Figure 1). Given a target overall FPR,  $F$  ( $\in (0, 1)$ ), PLBF optimizes  $\mathbf{t}$  ( $\in \mathbb{R}^{k+1}$ ) and  $\mathbf{f}$  ( $\in \mathbb{R}^k$ ) to minimize the total memory usage. Here,  $\mathbf{t}$  is a vector of thresholds for

---

**Algorithm 1** PLBF (Vaidya et al., 2021)

---

**Input:**

$\mathbf{g} \in \mathbb{R}^N$  : probabilities that the keys are contained in each segment  
 $\mathbf{h} \in \mathbb{R}^N$  : probabilities that the non-keys are contained in each segment  
 $F \in (0, 1)$  : target overall FPR  
 $k \in \mathbb{N}$  : number of regions

**Output:**

$\mathbf{t} \in \mathbb{R}^{k+1}$  : threshold boundaries of each region  
 $\mathbf{f} \in \mathbb{R}^k$  : FPRs of each region

**Algorithm:**

THRESMAXDIVDP( $\mathbf{g}, \mathbf{h}, j, k$ ) :  
 constructs  $\text{DP}_{\text{KL}}^j$  and calculates the optimal thresholds by tracing the transitions backward from  $\text{DP}_{\text{KL}}^j[j-1][k-1]$   
 OPTIMALFPR( $\mathbf{g}, \mathbf{h}, \mathbf{t}, F, k$ ) :  
 returns the optimal FPRs for each region under the given thresholds  
 SPACEUSED( $\mathbf{g}, \mathbf{h}, \mathbf{t}, \mathbf{f}$ ) :  
 returns the total size of the backup Bloom filters for the given thresholds and FPRs

MinSpaceUsed  $\leftarrow \infty$   
 $\mathbf{t}_{\text{best}} \leftarrow \text{None}$   
 $\mathbf{f}_{\text{best}} \leftarrow \text{None}$   
**for**  $j = k, k+1, \dots, N$   
    $\mathbf{t} \leftarrow \text{THRESMAXDIVDP}(\mathbf{g}, \mathbf{h}, j, k)$   
    $\mathbf{f} \leftarrow \text{OPTIMALFPR}(\mathbf{g}, \mathbf{h}, \mathbf{t}, F, k)$   
   **if** MinSpaceUsed  $>$  SPACEUSED( $\mathbf{g}, \mathbf{h}, \mathbf{t}, \mathbf{f}$ ) **then**  
     MinSpaceUsed  $\leftarrow$  SPACEUSED( $\mathbf{g}, \mathbf{h}, \mathbf{t}, \mathbf{f}$ )  
      $\mathbf{t}_{\text{best}} \leftarrow \mathbf{t}$   
      $\mathbf{f}_{\text{best}} \leftarrow \mathbf{f}$   
**return**  $\mathbf{t}_{\text{best}}, \mathbf{f}_{\text{best}}$

---

partitioning the score space into  $k$  regions, and  $\mathbf{f}$  is a vector of FPRs for each region, satisfying  $t_0 = 0 < t_1 < t_2 < \dots < t_k = 1$  and  $0 < f_i \leq 1$  ( $i = 1, 2, \dots, k$ ).

Next, we explain the optimization problem and its solution designed by PLBF. PLBF finds values of  $\mathbf{t}$  and  $\mathbf{f}$  that minimize the total memory usage of the backup Bloom filter, under the condition that the expected value of the overall FPR is  $F$ . Here, we define  $\mathbf{G} (\in \mathbb{R}^k)$  and  $\mathbf{H} (\in \mathbb{R}^k)$  as follows:

$$G_i = \Pr[t_i \leq s(x) < t_{i+1} | x \in \mathcal{S}], \quad H_i = \Pr[t_i \leq s(x) < t_{i+1} | x \in \mathcal{Q}]. \quad (2)$$

$G_i$  and  $H_i$  represent the probability that the score of a key and non-key, respectively, falls within the  $i$ -th region. Once  $\mathbf{t}$  is determined,  $\mathbf{G}$  and  $\mathbf{H}$  can be obtained using  $\mathcal{S}$ ,  $\mathcal{Q}$ , and the learned model. The expected value of the overall FPR is  $\sum_{i=1}^k H_i f_i$ . The total memory usage of the backup Bloom filter is given by  $\sum_{i=1}^k c|\mathcal{S}|G_i \log_2(1/f_i)$ , where  $c$  is a constant determined by the type of backup Bloom filters. Therefore, the optimization

---

**Algorithm 2** OptimalFPR (Algorithm 1 by Vaidya et al. (2021))
 

---

**Input:**

$\mathbf{G} \in \mathbb{R}^k$  : probabilities that the keys are contained in each region  
 $\mathbf{H} \in \mathbb{R}^k$  : probabilities that the non-keys are contained in each region  
 $F \in (0, 1)$  : target overall FPR  
 $k \in \mathbb{N}$  : number of regions

**Output:**

$\mathbf{f} \in \mathbb{R}^k$  : FPRs of each region

```

for  $i = 1, 2, \dots, k$ 
     $f_i \leftarrow G_i F / H_i$ 
while  $\exists i : f_i > 1$ 
     $G_{f=1} \leftarrow 0$ 
     $H_{f=1} \leftarrow 0$ 
    for  $i = 1, 2, \dots, k$ 
        if  $f_i \geq 1$  then
             $f_i \leftarrow 1$ 
             $G_{f=1} \leftarrow G_{f=1} + G_i$ 
             $H_{f=1} \leftarrow H_{f=1} + H_i$ 
    for  $i = 1, 2, \dots, k$ 
        if  $f_i < 1$  then
             $f_i \leftarrow ((F - H_{f=1})G_i) / ((1 - G_{f=1})H_i)$ 
return  $\mathbf{f}$ 
    
```

---

problem designed by PLBF is expressed as follows:

$$\begin{aligned}
 & \underset{\mathbf{f}, \mathbf{t}}{\text{minimize}} && \sum_{i=1}^k c|\mathcal{S}|G_i \log_2 \left( \frac{1}{f_i} \right) \\
 & \text{subject to} && \begin{cases} \sum_{i=1}^k H_i f_i \leq F \\ t_0 = 0 < t_1 < t_2 < \dots < t_k = 1 \\ f_i \leq 1 & (i = 1, 2, \dots, k). \end{cases}
 \end{aligned} \tag{3}$$

The original PLBF paper solved the problem by ignoring the condition  $f_i \leq 1$ . However, by introducing the set of indices  $\mathcal{I}_{f=1}$ , where  $f_i = 1$ , we can obtain a more general form of  $\mathbf{f}$  as follows (see the appendix for details):

$$f_i = \begin{cases} 1 & (i \in \mathcal{I}_{f=1}) \\ \frac{(F - H_{f=1})G_i}{(1 - G_{f=1})H_i} & (i \notin \mathcal{I}_{f=1}), \end{cases} \tag{4}$$

where

$$G_{f=1} = \sum_{i \in \mathcal{I}_{f=1}} G_i, \quad H_{f=1} = \sum_{i \in \mathcal{I}_{f=1}} H_i. \tag{5}$$

Then, the total backup Bloom filter memory usage, that is, the objective function of Equation (3), is

$$c|\mathcal{S}|(1 - G_{f=1}) \log_2 \left( \frac{1 - G_{f=1}}{F - H_{f=1}} \right) - c|\mathcal{S}| \sum_{i \notin \mathcal{I}_{f=1}} G_i \log_2 \left( \frac{G_i}{H_i} \right). \quad (6)$$

Next, we explain how PLBF finds the optimal  $\mathbf{t}$  and  $\mathbf{f}$ . PLBF divides the score space  $[0, 1]$  into  $N(> k)$  segments and then finds the optimal  $\mathbf{t}$  and  $\mathbf{f}$  using DP. Deciding how to cluster  $N$  segments into  $k$  consecutive regions corresponds to determining the threshold  $\mathbf{t}$  (Figure 2). We denote the probabilities that the key and non-key scores are contained in the  $i$ -th **segment** by  $g_i$  and  $h_i$ , respectively. Then, the probabilities that the key and non-key scores are contained in the  $i$ -th **region**, that is,  $G_i$  and  $H_i$ , are then calculated by summing the  $g$  and  $h$  values of the segments within each region (for example,  $g_1 + g_2 + g_3 = G_1$  in Figure 2).

PLBF makes the following assumption to find the optimal thresholds  $\mathbf{t}$ .

**Assumption 1** For optimal  $\mathbf{t}$  and  $\mathbf{f}$ ,  $\mathcal{I}_{f=1} = \emptyset$  or  $\mathcal{I}_{f=1} = \{k\}$ .

In other words, PLBF assumes that there is at most one region for which  $f = 1$ , and if there is one, it is the region with the highest score output by the machine learning model. Using this assumption, PLBF finds the optimal solution by trying all possible threshold values  $t_{k-1}$ . That is, PLBF finds the thresholds  $\mathbf{t}$  that minimize memory usage by solving the following problem for each  $j = k, k+1, \dots, N$ ; we find a way to cluster the 1st to  $(j-1)$ -th segments into  $k-1$  regions that maximizes

$$\sum_{i=1}^{k-1} G_i \log_2 \left( \frac{G_i}{H_i} \right). \quad (7)$$

PLBF solves this problem by building a  $j \times k$  DP table  $\text{DP}_{\text{KL}}^j[p][q]$  ( $p = 0, 1, \dots, j-1$  and  $q = 0, 1, \dots, k-1$ ) for each  $j = k, k+1, \dots, N$ ;  $\text{DP}_{\text{KL}}^j[p][q]$  denotes the maximum value of  $\sum_{i=1}^q G_i \log_2 (G_i/H_i)$  that can be obtained by clustering the 1st to  $p$ -th segments into  $q$  regions. To construct PLBF, one must find a clustering method that achieves  $\text{DP}_{\text{KL}}^j[j-1][k-1]$ .  $\text{DP}_{\text{KL}}^j$  can be computed recursively as follows:

$$\begin{aligned} & \text{DP}_{\text{KL}}^j[p][q] \quad (8) \\ = & \begin{cases} 0 & (p = 0 \wedge q = 0) \\ -\infty & ((p = 0 \wedge q > 0) \vee (p > 0 \wedge q = 0)) \\ \max_{i=1,2,\dots,p} \left( \text{DP}_{\text{KL}}^j[i-1][q-1] + d_{\text{KL}}(i,p) \right) & (\text{else}), \end{cases} \quad (9) \end{aligned}$$

where the function  $d_{\text{KL}}(i_l, i_r)$  is the following function defined for integers  $i_l$  and  $i_r$  satisfying  $1 \leq i_l \leq i_r \leq N$ :

$$d_{\text{KL}}(i_l, i_r) = \left( \sum_{i=i_l}^{i_r} g_i \right) \log_2 \left( \frac{\sum_{i=i_l}^{i_r} g_i}{\sum_{i=i_l}^{i_r} h_i} \right). \quad (10)$$



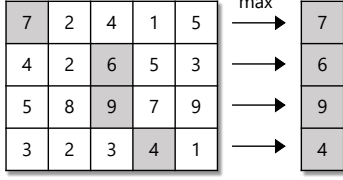


Figure 3: Example of a *matrix problem* for a *monotone matrix*.

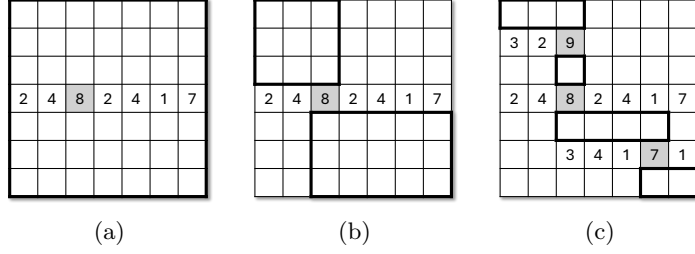


Figure 4: Monotone maxima. (a) exhaustive search on the middle row, and (b) narrowing the search area (c) are repeated recursively.

The time complexity to construct this DP table is  $\mathcal{O}(j^2k)$ . Then, by tracing the recorded transitions backward from  $\text{DP}_{\text{KL}}^j[j-1][k-1]$ , we obtain the best clustering with a time complexity of  $\mathcal{O}(k)$ . As the DP table is constructed for each  $j = k, k+1, \dots, N$ , the overall complexity is  $\mathcal{O}(N^3k)$ . We can divide the score space more finely with a larger  $N$  and thus obtain a  $\mathbf{t}$  closer to the optimum. However, the time complexity increases rapidly with increasing  $N$ .

We show the PLBF algorithm in Algorithm 1, and the OPTIMALFPR algorithm, which is used by PLBF, in Algorithm 2. For details of SPACEUSED, please refer to Equation (2) in the original PLBF paper (Vaidya et al., 2021). The worst case time complexity of OPTIMALFPR is  $\mathcal{O}(k^2)$  because this algorithm repeatedly solves the relaxation problem up to  $k$  times with a complexity of  $\mathcal{O}(k)$  until there are no more  $i$ s such that  $f_i > 1$ . The time complexity of SPACEUSED is  $\mathcal{O}(k)$ . As the DP table is constructed with a time complexity of  $\mathcal{O}(j^2k)$  for each  $j = k, k+1, \dots, N$ , the overall complexity is  $\mathcal{O}(N^3k)$ .

### 3.2 Matrix Problem

Here, we define the *matrix problem*, *monotone matrix*, and *totally monotone matrix* following Aggarwal et al. (1987).

**Definition 2 (*matrix problem*)** Let  $B$  be an  $n \times m$  real matrix, and let  $J : \{1, 2, \dots, n\} \rightarrow \{1, 2, \dots, m\}$  be a function defined on  $B$ . For each row index  $i$ ,  $J(i)$  denotes the smallest column index  $j$  such that  $B_{i,j}$  is the maximum value in the  $i$ -th row of  $B$ . Finding the value of  $J(i)$  for all  $i \in \{1, 2, \dots, n\}$  is called a *matrix problem*.

**Definition 3 (*monotone matrix*)** An  $n \times m$  real matrix  $B$  is called a *monotone matrix* if  $J(i) \leq J(i')$  for any  $i$  and  $i'$  that satisfy  $1 \leq i < i' \leq n$ .

**Definition 4 (*totally monotone matrix*)** An  $n \times m$  real matrix  $B$  is called a *totally monotone matrix* if every submatrix of  $B$  is monotone.

It is known that the definition of *totally monotone matrix* is equivalent to the following: all  $2 \times 2$  sub-matrices are monotone, that is, for any  $1 \leq i < i' \leq n$  and  $1 \leq j < j' \leq m$ ,  $A_{i,j} < A_{i,j'} \Rightarrow A_{i',j} < A_{i',j'}$  holds.

An example of a *matrix problem* for a *monotone matrix* is shown in Figure 3. Solving the *matrix problem* for a general  $n \times m$  matrix requires  $\mathcal{O}(nm)$  time complexity because all matrix values must be checked. Meanwhile, if the matrix is known to be a *monotone matrix*, the *matrix problem* for this matrix can be solved with time complexity of  $\mathcal{O}(n + m \log n)$  using the monotone maxima algorithm (Aggarwal et al., 1987). The exhaustive search for the middle row and the refinement of the search range are repeated recursively (Figure 4). In addition, the SMAWK algorithm can solve *matrix problem* in  $\mathcal{O}(n + m)$  for a *totally monotone matrix*. This algorithm efficiently solves *matrix problem* by recursively reducing the number of rows and columns to be considered, using the properties of completely monotonic matrices to maintain the necessary elements.

## 4 Methods

In this section, we propose three methods to speed up the construction of PLBF. First, we show that the computation of building the DP table  $\mathcal{O}(N)$  times in PLBF is redundant, and propose a method called fast PLBF that builds the DP table only one time and reuses it efficiently (Section 4.1). The computational complexity of building PLBF is  $\mathcal{O}(N^3k)$ , but fast PLBF is  $\mathcal{O}(N^2k)$ . We then propose fast PLBF++ (Section 4.2). In this method, we reduce the construction time to  $\mathcal{O}(Nk \log N)$  by (i) replacing OptimalFPR with a method that has a smaller worst-case computational complexity, and (ii) using the monotone maxima algorithm to speed up the construction of DP table. Finally, we propose fast PLBF# (Section 4.3). This algorithm reduces the construction time to  $\mathcal{O}(Nk \log k)$  by using the SMAWK algorithm instead of the monotone maxima. Although fast PLBF++ and fast PLBF# use approximations and do not necessarily achieve the same data structure as PLBF, we guarantee that, under an ideal condition, fast PLBF++ and fast PLBF# will have the same structure as PLBF. Additionally, we provide a theoretical guarantee for fast PLBF++ even in non-ideal conditions.

### 4.1 Fast PLBF

We propose fast PLBF, which constructs the same data structure as PLBF more quickly than PLBF by omitting the redundant construction of DP tables. Fast PLBF uses the same design as PLBF and finds the optimal  $\mathbf{t}$  and  $\mathbf{f}$  to minimize memory usage.

PLBF constructs a DP table for each  $j = k, k+1, \dots, N$ . We found that this computation is redundant and that we can also use the last DP table  $\text{DP}_{\text{KL}}^N$  for  $j = k, k+1, \dots, N-1$ . This is because the maximum value of  $\sum_{i=1}^{k-1} G_i \log_2 (G_i/H_i)$  when clustering the 1st to  $(j-1)$ -th segments into  $k-1$  regions is equal to  $\text{DP}_{\text{KL}}^N[j-1][k-1]$ . We can obtain the best clustering by tracing the transitions backward from  $\text{DP}_{\text{KL}}^N[j-1][k-1]$ . The time complexity of tracing the transitions is  $\mathcal{O}(k)$ , which is faster than constructing the DP table.

The pseudo-code for fast PLBF construction is provided in Algorithm 3. The time complexity of building  $\text{DP}_{\text{KL}}^N$  is  $\mathcal{O}(N^2k)$ , and the worst-case complexity of subsequent computations is  $\mathcal{O}(Nk^2)$ . Because  $N > k$ , the total complexity is  $\mathcal{O}(N^2k)$ , which is faster than  $\mathcal{O}(N^3k)$  for PLBF, although fast PLBF constructs the same data structure as PLBF.

---

**Algorithm 3** Fast PLBF
 

---

**Algorithm:**

```

    MAXDIVDP( $\mathbf{g}, \mathbf{h}, N, k$ ) :
        constructs  $\text{DP}_{\text{KL}}^N$ 
    THRESMAXDIV( $\text{DP}_{\text{KL}}^N, j, k$ ) :
        traces the transitions backward from  $\text{DP}_{\text{KL}}^N[j-1][k-1]$  and finds the optimal thresholds

    MinSpaceUsed  $\leftarrow \infty$ 
     $\mathbf{t}_{\text{best}} \leftarrow \text{None}$ 
     $\mathbf{f}_{\text{best}} \leftarrow \text{None}$ 
     $\text{DP}_{\text{KL}}^N \leftarrow \text{MAXDIVDP}(\mathbf{g}, \mathbf{h}, N, k)$ 
    for  $j = k, k+1, \dots, N$ 
         $\mathbf{t} \leftarrow \text{THRESMAXDIV}(\text{DP}_{\text{KL}}^N, j, k)$ 
         $\mathbf{f} \leftarrow \text{OPTIMALFPR}(\mathbf{g}, \mathbf{h}, \mathbf{t}, F, k)$ 
        if MinSpaceUsed > SPACEUSED( $\mathbf{g}, \mathbf{h}, \mathbf{t}, \mathbf{f}$ ) then
            MinSpaceUsed  $\leftarrow \text{SPACEUSED}(\mathbf{g}, \mathbf{h}, \mathbf{t}, \mathbf{f})$ 
             $\mathbf{t}_{\text{best}} \leftarrow \mathbf{t}$ 
             $\mathbf{f}_{\text{best}} \leftarrow \mathbf{f}$ 
    return  $\mathbf{t}_{\text{best}}, \mathbf{f}_{\text{best}}$ 
    
```

---

## 4.2 Fast PLBF++

We propose fast PLBF++, which can be constructed even faster than fast PLBF. The acceleration of fast PLBF++ consists of two components. First, fast PLBF++ improves the worst-case computational complexity of OPTIMALFPR, the algorithm for finding the optimal FPR for each backup Bloom filter (Section 4.2.1). Second, fast PLBF++ accelerates the construction of the DP table  $\text{DP}_{\text{KL}}^N$ , that is, MAXDIVDP, by taking advantage of a characteristic that DP tables often have (Section 4.2.2). We provide theoretical guarantees on the memory efficiency of fast PLBF++ under both ideal conditions (Section 4.2.3) and non-ideal conditions (Section 4.2.4).

### 4.2.1 SPEED UP OPTIMALFPR

We improve the worst-case complexity of PLBF's OPTIMALFPR from  $\mathcal{O}(k^2)$  to  $\mathcal{O}(k \log k)$ . The original OPTIMALFPR algorithm repeatedly solves the relaxation problem, where the condition  $f_i \leq 1$  is ignored, until there are no more  $i$  satisfying  $f_i > 1$ . Since each iteration takes a complexity of  $\mathcal{O}(k)$  and the repetition is at most  $k$  times, the worst-case complexity of the original OPTIMALFPR algorithm is  $\mathcal{O}(k^2)$ . However, by carefully analyzing the optimization problem, we can improve the worst-case complexity to  $\mathcal{O}(k \log k)$ .

First, we prove the following theorem.

**Theorem 5** *There exists an optimal solution  $\mathbf{f}$  to the optimization problem (Equation 3) that satisfies*

$$\frac{G_i}{H_i} < \frac{G_j}{H_j} \quad (11)$$

for all  $i, j$  such that  $f_i < 1, f_j = 1$ . (Here, when  $H_i = 0, G_i/H_i = \infty$ , which is greater than any finite value.)

**Proof** First, in the case of  $\sum_{i \in \{j | G_j > 0\}} H_i \leq F$ , one of the optimal solution  $\mathbf{f}$  is

$$f_i = \begin{cases} 0 & (G_i = 0) \\ 1 & (G_i > 0), \end{cases} \quad (12)$$

and it is clear that the claim holds.

Otherwise, in the case of  $\sum_{i \in \{j | G_j > 0\}} H_i > F$ , from Equation (71), Equation (72), and Equation (73), there exists an optimal solution  $\mathbf{f}$  and a threshold  $T (\in \mathbb{R})$  that satisfy

$$H_i = 0 \Rightarrow f_i = 1, \quad (13)$$

$$H_i > 0 \wedge \frac{G_i}{H_i} \geq T \Rightarrow f_i = 1, \quad (14)$$

$$H_i > 0 \wedge \frac{G_i}{H_i} < T \Rightarrow f_i < 1. \quad (15)$$

Therefore, it is clear that the claim holds. ■

This theorem indicates that only some  $i$  with the highest  $G_i/H_i$  are included in the set  $\mathcal{I}_{f=1}$ . As a result, there are at most  $k$  potential candidate sets  $\mathcal{I}_{f=1}$  that could form the optimal solution.

To find the optimal set, we first sort the values of  $G_i/H_i$  in descending order. This sorting operation has a worst-case time complexity of  $\mathcal{O}(k \log k)$ . Once sorted, we evaluate the objective function for each candidate set  $\mathcal{I}_{f=1}$  sequentially. To do this efficiently, we maintain and update the following values as we examine each candidate set:  $G_{f=1} (= \sum_{i \in \mathcal{I}_{f=1}} G_i)$ ,  $H_{f=1} (= \sum_{i \in \mathcal{I}_{f=1}} H_i)$ , and  $\sum_{i \notin \mathcal{I}_{f=1}} G_i \log_2 (G_i/H_i)$ . This allows us to evaluate Equation (6) in  $\mathcal{O}(1)$  time for each candidate set. Therefore, the total worst-case complexity is  $\mathcal{O}(k \log k)$ .

#### 4.2.2 SPEED UP MAXDIVDP

Fast PLBF++ speed up MAXDIVDP based on the following intuition; it is more likely that when the number of regions is fixed at  $q$  and the number of segments is increased by 1, the optimal  $t_{q-1}$  remains unchanged or increases, as in Figure 5(a), than that  $t_{q-1}$  decreases, as in Figure 5(b). Fast PLBF++ takes advantage of this characteristic to construct the DP table with less complexity  $\mathcal{O}(Nk \log N)$ .

First, we define the terms to describe fast PLBF++. For simplicity,  $\text{DP}_{\text{KL}}^N$  is denoted as  $\text{DP}_{\text{KL}}$  in this section. The  $(N-1) \times (N-1)$  matrix  $A$  is defined as follows:

$$A_{p,i} = \begin{cases} \text{DP}_{\text{KL}}[i-1][q-1] + d_{\text{KL}}(i,p) & (i = 1, 2, \dots, p) \\ -\infty & (\text{else}). \end{cases} \quad (16)$$

Then, from the definition of  $\text{DP}_{\text{KL}}$ ,

$$\text{DP}_{\text{KL}}[p][q] = \max_{i=1,2,\dots,N-1} A_{p,i}. \quad (17)$$

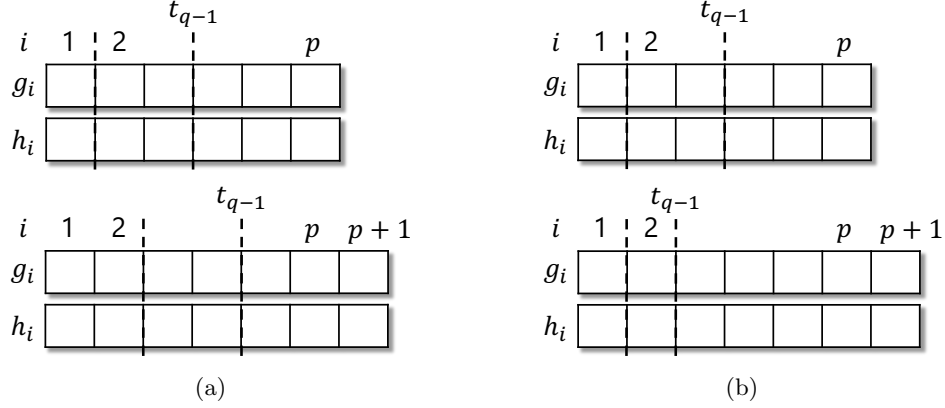


Figure 5: When the number of regions is fixed at  $q$  and the number of segments is increased by 1, the optimal  $t_{q-1}$  remains unchanged or increases if  $A$  is a *monotone matrix* (a). When  $A$  is not a *monotone matrix* (b), the optimal  $t_{q-1}$  may decrease.

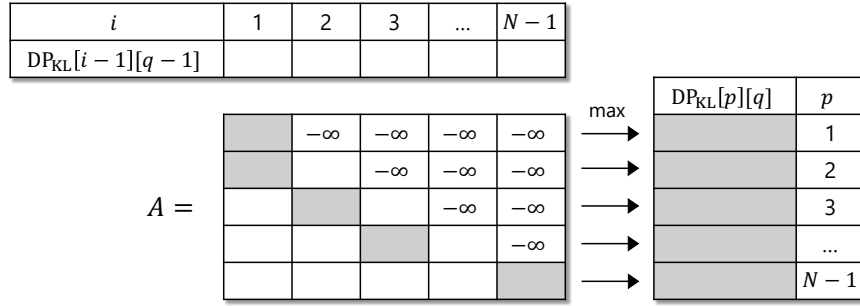


Figure 6: Computing  $DP_{KL}[p][q]$  ( $p = 1, 2, \dots, N-1$ ) from  $DP_{KL}[p][q-1]$  ( $p = 0, 1, \dots, N-2$ ) via the matrix  $A$ . The computation is the same as solving the *matrix problem* for matrix  $A$ . When the score distribution is *ideal*,  $A$  is a *monotone matrix*.

The matrix  $A$  represents the intermediate calculations involved in determining  $DP_{KL}[p][q]$  from  $DP_{KL}[p][q-1]$  (Figure 6). When the intuition that  $t_{q-1}$  does not decrease, as discussed at the beginning of this section, holds,  $A$  is a *monotone matrix*.

While fast PLBF checks almost all elements of the matrix  $A$  and thus takes  $\mathcal{O}(N^2)$  computations, fast PLBF++ uses the monotone maxima algorithm to obtain an approximation of the maximum value of each row of the matrix  $A$  in  $\mathcal{O}(N \log N)$  computations. This is much faster than PLBF and fast PLBF, but it involves certain approximations, so it does not necessarily achieve the same optimal memory efficiency as those methods.

#### 4.2.3 THEORETICAL GUARANTEES UNDER IDEAL CONDITIONS

Here, we demonstrate that the memory efficiency of fast PLBF++ is equivalent to that of PLBF under ideal conditions. The acceleration of fast PLBF++ is attributed to two

factors. The first factor, speed up OPTIMALFPR, involves no approximation, so we focus on proving that there is no degradation due to approximation in the second factor, speed up MAXDIVDP, under ideal conditions.

First, we define an *ideal score distribution* as follows.

**Definition 6** *A score distribution is called ideal if*

$$\frac{g_1}{h_1} \leq \frac{g_2}{h_2} \leq \dots \leq \frac{g_N}{h_N}. \quad (18)$$

An *ideal score distribution* implies that the probability of  $x \in \mathcal{S}$  and the score  $s(x)$  are ideally well correlated. In other words, an *ideal score distribution* means that the machine learning model learns the distribution ideally.

Fast PLBF++ does not necessarily have the same data structure as PLBF because  $A$  is not necessarily a *monotone matrix*. However, as the following theorem shows, we can prove that  $A$  is a *monotone matrix* and thus fast PLBF++ has the same data structure as (fast) PLBF under certain conditions.

First, the following lemma holds.

**Lemma 7** *If the score distribution is ideal, then for all  $1 \leq i < i' \leq p < p' \leq N$ , it holds that*

$$(d_{\text{KL}}(i, p) + d_{\text{KL}}(i', p')) - (d_{\text{KL}}(i, p') + d_{\text{KL}}(i', p)) \geq 0. \quad (19)$$

**Proof** We define  $u_1, u_2, v_1, v_2, x$ , and  $y$  as follows:

$$\begin{aligned} u_1 &:= \sum_{j=i'}^p g_j, & u_2 &:= \sum_{j=i}^p g_j, & x &:= \sum_{j=p+1}^{p'} g_j, \\ v_1 &:= \sum_{j=i'}^p h_j, & v_2 &:= \sum_{j=i}^p h_j, & y &:= \sum_{j=p+1}^{p'} h_j. \end{aligned} \quad (20)$$

Here, we define the left-hand side of Equation (19) as the function  $D(x, y)$ , that is,

$$D(x, y) \quad (21)$$

$$:= (d_{\text{KL}}(i, p) + d_{\text{KL}}(i', p')) - (d_{\text{KL}}(i, p') + d_{\text{KL}}(i', p)) \quad (22)$$

$$= \left( u_2 \log_2 \left( \frac{u_2}{v_2} \right) + (u_1 + x) \log_2 \left( \frac{u_1 + x}{v_1 + y} \right) \right) - \quad (23)$$

$$\left( (u_2 + x) \log_2 \left( \frac{u_2 + x}{v_2 + y} \right) + u_1 \log_2 \left( \frac{u_1}{v_1} \right) \right). \quad (24)$$

Since the score distribution is *ideal*, we have  $(u_2 + x)/(v_2 + y) \leq (u_1 + x)/(v_1 + y)$ . Therefore,

$$\frac{\partial D}{\partial x} = \log_2 \left( \frac{u_1 + x}{v_1 + y} \right) - \log_2 \left( \frac{u_2 + x}{v_2 + y} \right) \geq 0, \quad (25)$$

$$\frac{\partial D}{\partial y} = \left( -\frac{u_1 + x}{v_1 + y} + \frac{u_2 + x}{v_2 + y} \right) \log_2(e) \leq 0. \quad (26)$$

Since the score distribution is *ideal*, we also have  $u_1/v_1 \leq x/y$ . Thus,

$$D(x, y) \geq \inf_{0 < x, 0 < y, \frac{u_1}{v_1} \leq \frac{x}{y}} D(x, y) \quad (27)$$

$$\geq \inf_{0 < x, 0 < y, \frac{u_1}{v_1} = \frac{x}{y}} D(x, y). \quad (28)$$

When  $\frac{u_1}{v_1} = \frac{x}{y}$ , we can introduce a positive variable  $z$  such that  $x = zu_1$  and  $y = zv_1$ . Substituting this into the expression, we have

$$D(x, y) \geq \inf_{z > 0} D(zu_1, zv_1) \quad (29)$$

$$= \inf_{z > 0} \left( zu_1 \log_2 \left( \frac{zu_1}{zv_1} \right) + u_2 \log_2 \left( \frac{u_2}{v_2} \right) - (zu_1 + u_2) \log_2 \left( \frac{zu_1 + u_2}{zv_1 + v_2} \right) \right). \quad (30)$$

Finally, by applying Jensen's inequality (Jensen, 1906), we obtain  $D(x, y) \geq 0$ .  $\blacksquare$

Using Lemma 7, we can prove the following theorem, which demonstrates that the memory efficiency of fast PLBF++ is equivalent to that of PLBF when the score distribution is *ideal*.

**Theorem 8** *If the score distribution is ideal,  $A$  is a totally monotone matrix.*

**Proof**

For any  $i, i', p, p'$  satisfying  $1 \leq i < i' \leq p < p' \leq N - 1$ ,

$$(A_{p,i} + A_{p',i'}) - (A_{p',i} + A_{p,i'}) \quad (31)$$

$$= ((\text{DP}_{\text{KL}}[i-1][q-1] + d_{\text{KL}}(i, p)) + (\text{DP}_{\text{KL}}[i'-1][q-1] + d_{\text{KL}}(i', p'))) - \quad (32)$$

$$((\text{DP}_{\text{KL}}[i-1][q-1] + d_{\text{KL}}(i, p')) + (\text{DP}_{\text{KL}}[i'-1][q-1] + d_{\text{KL}}(i', p))) \quad (33)$$

$$= (d_{\text{KL}}(i, p) + d_{\text{KL}}(i', p')) - (d_{\text{KL}}(i, p') + d_{\text{KL}}(i', p)) \quad (34)$$

$$\geq 0. \quad (35)$$

The last inequality is from the Lemma 7. Thus,  $A_{p,i} < A_{p',i'} \Rightarrow A_{p',i} < A_{p,i'}$  holds. Consequently, it has been demonstrated that every  $2 \times 2$  submatrix is monotone, thereby proving that  $A$  is a *totally monotone matrix*.  $\blacksquare$

#### 4.2.4 THEORETICAL GUARANTEES UNDER NON-IDEAL CONDITIONS

Here, we provide a theoretical guarantee for cases where the distribution is not *ideal*. Specifically, we offer an upper bound on the difference in  $\text{DP}_{\text{KL}}$  between solving the matrix problem greedily and solving it efficiently using monotone maxima. For simplicity, we will assume that  $N = 2^M$  ( $M \in \mathbb{N}$ ). In this case, when selecting the “middle row” in the monotone maxima algorithm, the number of rows to be considered will always be odd, allowing us to choose the exact middle row. For example, in Figure 4, the number of rows is 7, corresponding to the case of  $N = 8 = 2^3$ .

First, we define the function  $\Delta : \{0, 1, \dots, N\} \times \{0, 1, \dots, N\} \rightarrow \mathbb{R}$  as follows:

$$\Delta(p, p') \tag{36}$$

$$= \begin{cases} \max_{1 \leq i \leq i' \leq p} - (d_{\text{KL}}(i, p) + d_{\text{KL}}(i', p')) + (d_{\text{KL}}(i, p') + d_{\text{KL}}(i', p)) & (0 < p < p' < N) \\ 0 & (\text{else}). \end{cases} \tag{37}$$

From Lemma 7, when the distribution is *ideal*,  $\Delta(p, p') \leq 0$  for any  $p, p'$ . Furthermore, we define  $\delta : \{0, 1, \dots, N\} \rightarrow \mathbb{R}$  recursively as follows:

$$\delta(p) = \begin{cases} 0 & (p = 0, N) \\ \max(\delta(l) + \Delta(l, p), 0, \delta(r) + \Delta(p, r)) & (\text{else}). \end{cases} \tag{38}$$

In this definition,  $l$  is the largest row index smaller than  $p$  that has been processed before the  $p$ -th row by the monotone maxima algorithm (if no such row exists, we set  $l = 0$ ). Similarly,  $r$  is the smallest row index greater than  $p$  that has been processed before the  $p$ -th row by the monotone maxima algorithm (if no such row exists, we set  $r = N$ ). For example, when  $N = 8$ , as shown in Figure 4, we have  $l = 2$  and  $r = 4$  for  $p = 3$ ,  $l = 0$  and  $r = 8$  for  $p = 4$ . Since  $N = 2^M$  ( $M \in \mathbb{N}$ ), we have  $l = p - 2^m$  and  $r = p + 2^m$ , where  $m$  is the largest non-negative integer such that  $p$  is divisible by  $2^m$ . Then, we define  $\delta_{\max}$  as follows:

$$\delta_{\max} = \max_{p=1,2,\dots,N-1} \delta(p). \tag{39}$$

$\delta_{\max}$  is a value that depends on the training data and  $N$ . In particular, when the distribution is *ideal*,  $\delta(p) = 0$  for all  $p$ , and therefore,  $\delta_{\max} = 0$ .

Here, the following theorem holds.

**Theorem 9** *Let  $\text{DP}_{\text{true}}$  be the  $\text{DP}_{\text{KL}}$  in the case of (fast) PLBF, that is, when calculating greedily without using monotone maxima. Furthermore, let  $\text{DP}_{\text{mm}}$  be the  $\text{DP}_{\text{KL}}$  in the case of fast PLBF++, that is, when calculating with monotone maxima. Then, for all  $p = 1, 2, \dots, N - 1$  and  $q = 1, 2, \dots, k - 1$ ,*

$$0 \leq \text{DP}_{\text{true}}[p][q] - \text{DP}_{\text{mm}}[p][q] \leq q\delta_{\max}. \tag{40}$$

**Proof**  $\text{DP}_{\text{true}}[p][q]$  is a DP table derived from the exact calculation of all transitions, whereas  $\text{DP}_{\text{mm}}[p][q]$  is a DP table derived from calculations where some transitions are omitted. Therefore, it is evident that  $0 \leq \text{DP}_{\text{true}}[p][q] - \text{DP}_{\text{mm}}[p][q]$ . We will now prove the right-hand side of the inequality.

As the definition in Theorem 2, let  $J(p)$  be the smallest column index  $j$  such that  $A_{p,j}$  is the maximum value in the  $p$ -th row of  $A$ . Additionally, let  $\hat{J}(p)$  be the column index  $j$  such that the monotone maximum algorithm considers  $A_{p,j}$  to be the maximum value in the  $p$ -th row of  $A$ .  $J(p)$  and  $\hat{J}(p)$  always satisfy  $A_{p,J(p)} - A_{p,\hat{J}(p)} \geq 0$ .

First, we prove recursively that  $A_{p,J(p)} - A_{p,\hat{J}(p)} \leq \delta(p)$  for all  $p = 1, 2, \dots, N - 1$ . We introduce virtual 0-th and  $N$ -th row to the matrix  $A$ , and we assume  $J(0) = \hat{J}(0) = 0$ ,  $J(N) = \hat{J}(N) = N - 1$ , and  $A_{0,J(0)} - A_{0,\hat{J}(0)} = A_{N,J(N)} - A_{N,\hat{J}(N)} = 0$ . Now, assume that for all  $q$  ( $\in \{0, 1, \dots, N\}$ ) that is a multiple of  $2^{m+1}$ ,  $A_{q,J(q)} - A_{q,\hat{J}(q)} \leq \delta(q)$  holds.



This assumption is clearly true when  $m + 1 = M$  because  $N = 2^M$  and we introduced the virtual 0-th and  $N$ -th row. Then, we can prove that for any  $p \in \{0, 1, \dots, N\}$  that is a multiple of  $2^m$ ,  $A_{p,J(p)} - A_{p,\hat{J}(p)} \leq \delta(p)$  holds. In the following, let  $p$  be a number that is a multiple of  $2^m$ , but not a multiple of  $2^{m+1}$ . In this case,  $l = p - 2^m$  and  $r = p + 2^m$ , where the range of indices to be searched by the monotone maximum algorithm in the  $p$ -th row is determined by the search result of the  $l$ -th and  $r$ -th rows. We denote the minimum and maximum values of this range of indices as  $L(p)$  and  $R(p)$ , which can be expressed as follows:

$$L(p) = \begin{cases} 1 & (l = 0) \\ \hat{J}(l) & (\text{else}) \end{cases}, \quad R(p) = \begin{cases} N - 1 & (r = N) \\ \hat{J}(r) & (\text{else}). \end{cases} \quad (41)$$

First, from the definition of  $\hat{J}(p)$ ,

$$\max_{L(p) \leq j \leq R(p)} A_{p,j} - A_{p,\hat{J}(p)} = A_{p,\hat{J}(p)} - A_{p,\hat{J}(p)} = 0. \quad (42)$$

Next, when  $R(p) < p$ ,

$$\max_{R(p) < j \leq p} A_{p,j} - A_{p,\hat{J}(p)} \leq \max_{R(p) < j \leq p} A_{p,j} - A_{p,\hat{J}(r)} \quad (43)$$

$$\leq \max_{R(p) < j \leq p} A_{r,j} - A_{r,\hat{J}(r)} + \Delta(p, r) \quad (44)$$

$$\leq A_{r,J(r)} - A_{r,\hat{J}(r)} + \Delta(p, r) \quad (45)$$

$$\leq \delta(r) + \Delta(p, r). \quad (46)$$

Here, the first and third inequality is due to  $A_{p,\hat{J}(p)} = \max_{\hat{J}(l) \leq j \leq \hat{J}(r)} A_{p,j} \geq A_{p,\hat{J}(r)}$  and  $A_{r,J(r)} = \max_{1 \leq j \leq r} A_{r,j} \geq A_{r,\hat{J}(r)}$ . The fourth inequality is based on the assumptions of induction (note that  $r$  is multiple of  $2^{m+1}$ ). The second inequality can be shown as follows, using the definition of  $A$  and  $\Delta$ :

$$\max_{\hat{J}(r) < j \leq p} A_{p,j} - A_{p,\hat{J}(r)} \quad (47)$$

$$= \max_{\hat{J}(r) < j \leq p} (\text{DP}_{\text{KL}}[j - 1][q - 1] + d_{\text{KL}}(j, p)) - \quad (48)$$

$$(\text{DP}_{\text{KL}}[\hat{J}(r) - 1][q - 1] + d_{\text{KL}}(\hat{J}(r), p)) \quad (49)$$

$$\leq \max_{\hat{J}(r) < j \leq p} (\text{DP}_{\text{KL}}[j - 1][q - 1] + d_{\text{KL}}(j, r)) - \quad (50)$$

$$(\text{DP}_{\text{KL}}[\hat{J}(r) - 1][q - 1] + d_{\text{KL}}(\hat{J}(r), r)) + \Delta(p, r) \quad (51)$$

$$= \max_{\hat{J}(r) < j \leq p} A_{r,j} - A_{r,\hat{J}(r)} + \Delta(p, r). \quad (52)$$

In the same way, we have

$$\max_{1 \leq j < L(p)} A_{p,j} - A_{p,\hat{J}(p)} \leq \delta(l) + \Delta(l, p). \quad (53)$$

Therefore, from Equation (53), Equation (42), and Equation (46),

$$A_{p,J(p)} - A_{p,j(p)} = \max_{1 \leq j \leq p} A_{p,j} - A_{p,j(p)} \quad (54)$$

$$\leq \max(\delta(l) + \Delta(l, p), 0, \delta(r) + \Delta(p, r)) \quad (55)$$

$$= \delta(p). \quad (56)$$

Thus, we have  $A_{p,J(p)} - A_{p,j(p)}$  for all  $p \in \{1, 2, \dots, N-1\}$ . This means that a deviation up to  $\delta_{\max}$  is produced in row to row calculation in DP table. Therefore, it has been shown that the maximum error in  $\text{DP}_{\text{KL}}[p][q]$  is  $q\delta_{\max}$ .  $\blacksquare$

Since  $\delta_{\max} = 0$  when the distribution is *ideal*, the DP table generated in the fast PLBF++ construction is exactly the same as the DP table generated in the fast PLBF construction. The conclusion from Theorem 8 covers only *ideal* situations. However, Theorem 9 theoretically bounds the difference even in *non-ideal* situations by using  $\delta_{\max}$ , a value that, in a sense, indicates the deviation from the *ideal* distribution. The URL and malware data sets we used for our experiment have  $\delta_{\max} = 0.028$  and  $\delta_{\max} = 0.010$ , respectively, when  $N = 1024$ . Considering  $k \sim 10$ , which is a typical setting, the difference in the DP table value is approximately up to 0.25. If  $\mathcal{I}_{f=1} = \emptyset$ , this suggests that the difference in memory usage between fast PLBF and fast PLBF++ is at most  $0.25 \times \log_2(e) = 0.36$  bit per element. Additionally, it implies that for the same memory usage, the difference in the FPR is at most  $2^{0.25} = 1.18$  times.

### 4.3 Fast PLBF#

Fast PLBF# uses the SMAWK algorithm instead of the monotone maxima. In addition, as with fast PLBF++, it replaces `OPTIMALFPR` with `FASTOPTIMALFPR`, which has better worst-case computational complexity. Therefore, the DP using the SMAWK algorithm takes  $\mathcal{O}(Nk)$  time, and for each of the  $j = k, k+1, \dots, N$ , determining the optimal FPR takes  $\mathcal{O}(k \log k)$  operations, so the overall time taken is  $\mathcal{O}(Nk) + \mathcal{O}(Nk \log k) = \mathcal{O}(Nk \log k)$ .

The SMAWK algorithm is an algorithm that solves the problem of finding the maximum value of each row of a matrix. While monotone maxima assumes that the matrix is a *monotone matrix*, the SMAWK algorithm assumes that the matrix is a *totally monotone matrix*. The *totally monotone* assumption is stronger than the *monotone* assumption, that is, every *totally monotone matrix* is a *monotone matrix*. Therefore, the SMAWK algorithm is an algorithm that relies on stronger assumptions than those of monotone maxima. Although the SMAWK algorithm is more complicated than monotone maxima, it has less computational complexity.

From the proof of Theorem 8,  $A$  is a *totally monotone matrix* when the distribution is *ideal*. Therefore, although the SMAWK algorithm relies on stronger assumptions than monotone maxima, it satisfies the assumptions of both algorithms under the condition that the distribution is *ideal*. As we will see in the next section, fast PLBF# achieves almost the same memory efficiency as (fast) PLBF, just as fast PLBF++ does.

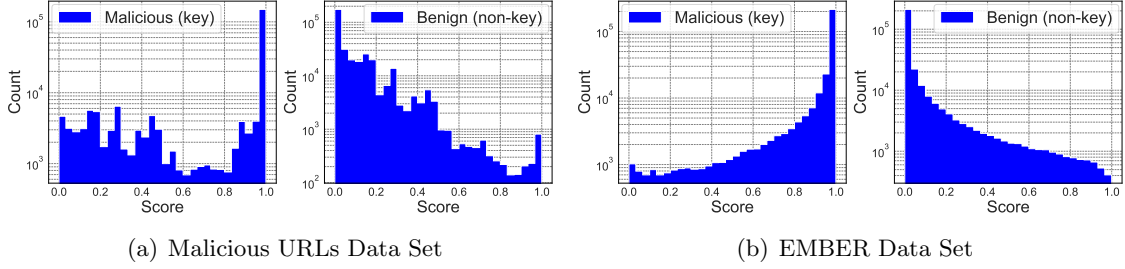


Figure 7: Histograms of the score distributions of keys and non-keys.

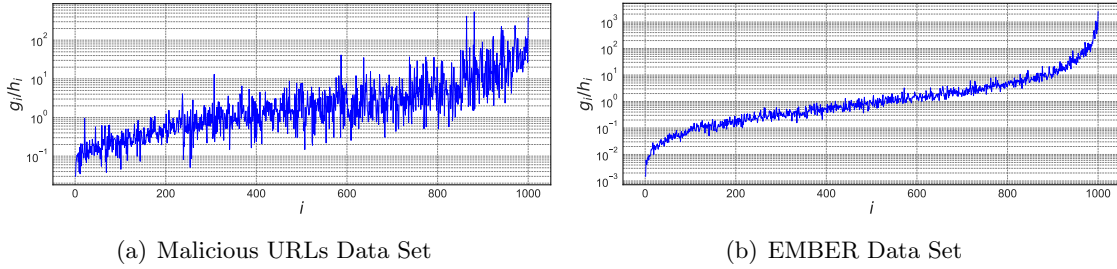


Figure 8: Ratio of keys to non-keys.

## 5 Experimentns

This section evaluates the experimental performance of fast PLBF, fast PLBF++, and fast PLBF#. We compared the performances of our proposed methods with four baselines: Bloom filter (Bloom, 1970), Ada-BF (Dai and Shrivastava, 2020), sandwiched LBF (Mitzenmacher, 2018), and PLBF (Vaidya et al., 2021). Similar to PLBF, Ada-BF is an LBF that partitions the score space into several regions and assigns different FPRs to each region. However, Ada-BF relies heavily on heuristics for clustering and assigning FPRs. Sandwiched LBF is a LBF that “sandwiches” a machine learning model with two Bloom filters. This achieves better memory efficiency than the original LBF by optimizing the size of two Bloom filters.

To facilitate the comparison of different methods or hyperparameters results, we have slightly modified the original PLBF framework. The original PLBF was designed to minimize memory usage under the condition of a given FPR. However, this approach makes it difficult to compare the results of different methods or hyperparameters. This is because both the FPR at test time and the memory usage vary depending on the method and hyperparameters, which often makes it difficult to determine the superiority of the results. Therefore, in our experiments, we used a framework where the expected FPR is minimized under the condition of memory usage. This makes it easy to obtain two results with the same memory usage and compare them by the FPR at test time. See the appendix for more information on how this framework modification will change the construction method of PLBFs.

We evaluated the algorithms using the following two data sets.

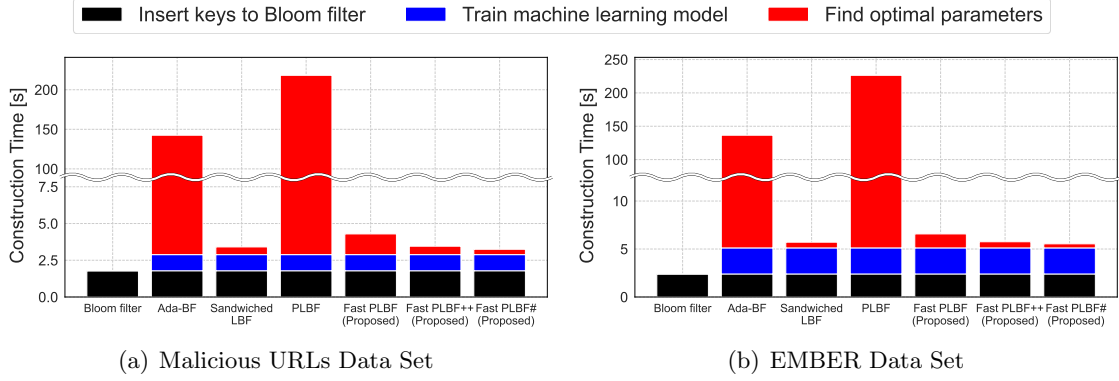


Figure 9: Construction time.

- **Malicious URLs Data Set:** As in previous papers (Dai and Shrivastava, 2020; Vaidya et al., 2021), we used Malicious URLs data set (Siddhartha, 2021). The URLs data set comprises 223,088 malicious and 428,118 benign URLs. We extracted 20 lexical features such as URL length, use of shortening, number of special characters, etc. We used all malicious URLs and 342,482 (80%) benign URLs as the training set, and the remaining benign URLs as the test set.
- **EMBER Data Set:** We used the EMBER data set (Anderson and Roth, 2018) as in the PLBF research. The data set consists of 300,000 malicious and 400,000 benign files, along with the features of each file. We used all malicious files and 300,000 (75%) benign files as the train set and the remaining benign files as the test set.

While any model can be used for the classifier, we used LightGBM (Ke et al., 2017) because of its fast training and inference, memory efficiency, and accuracy. The sizes of the machine learning model for the URLs and EMBER data sets are 312 Kb and 1.19 Mb, respectively. The training time of the machine learning model for the URLs and EMBER data sets is 1.09 and 2.71 seconds, respectively. The memory usage of LBF is the memory usage of the backup Bloom filters plus the size of the machine learning model. Figure 7 shows a histogram of the score distributions for keys and non-keys in each data set. We can see that the frequency of keys increases and that of non-keys decreases as the score increases. In addition, Figure 8 plots  $g_i/h_i$  ( $i = 1, 2, \dots, N$ ) when  $N = 1,000$ . We can see that  $g_i/h_i$  tends to increase as  $i$  increases, but the increase is not monotonic; that is, the score distribution is not *ideal*.

### 5.1 Construction Time

We compared the construction times of our proposed methods with those of existing methods. Following the experiments in the original PLBF paper, hyperparameters for PLBFs were set to  $N = 1,000$  and  $k = 5$ .

Figure 9 shows the construction time for each method. The construction time for LBFs includes not only the time to insert keys into the Bloom filters but also the time to train

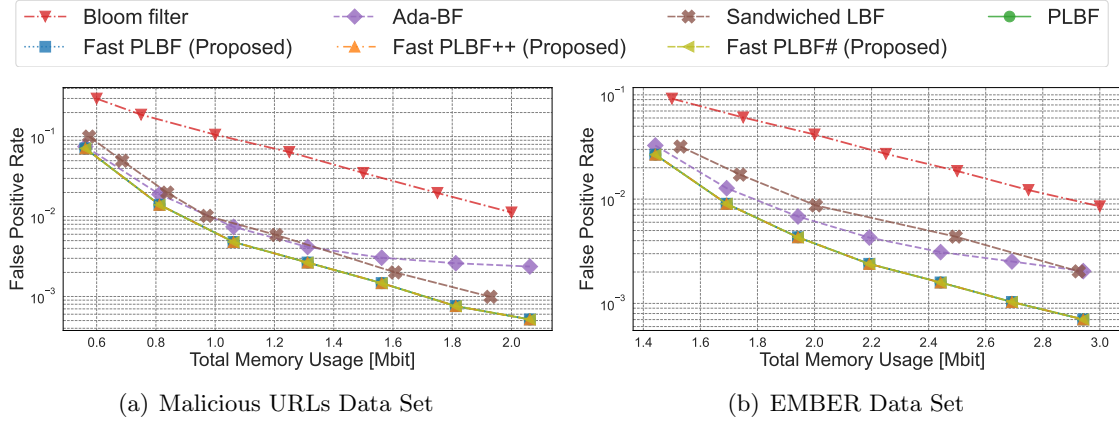


Figure 10: Trade-off between memory usage and FPR.

the machine learning model and the time to compute the optimal parameters ( $\mathbf{t}$  and  $\mathbf{f}$  in the case of PLBF).

Ada-BF and sandwiched LBF use heuristics to find the optimal parameters, so they have shorter construction times than PLBF. However, these methods demonstrate lower accuracy, as we will demonstrate in the following section. PLBF has better accuracy but takes more than 3 minutes to find the optimal  $\mathbf{t}$  and  $\mathbf{f}$ . On the other hand, our proposed methods take less than 2 seconds. Specifically, fast PLBF constructs 50.8 and 34.3 times faster than PLBF for the URLs and EMBER data sets, respectively. Fast PLBF++ and fast PLBF# exhibit even greater speed improvements; fast PLBF++ is 63.1 and 39.3 times faster, and fast PLBF# is 67.2 and 40.8 times faster than PLBF for the URLs and EMBER data sets, respectively. These construction times are comparable to those of sandwiched LBF, which relies heavily on heuristics and, as we will see in the next section, is much less accurate than PLBF.

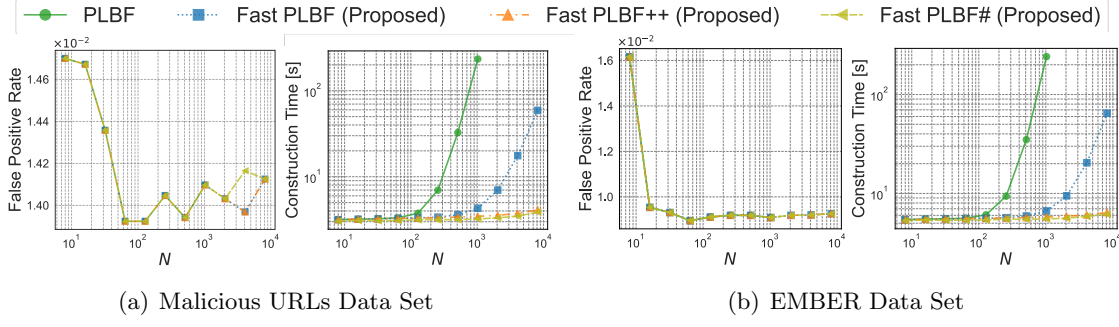
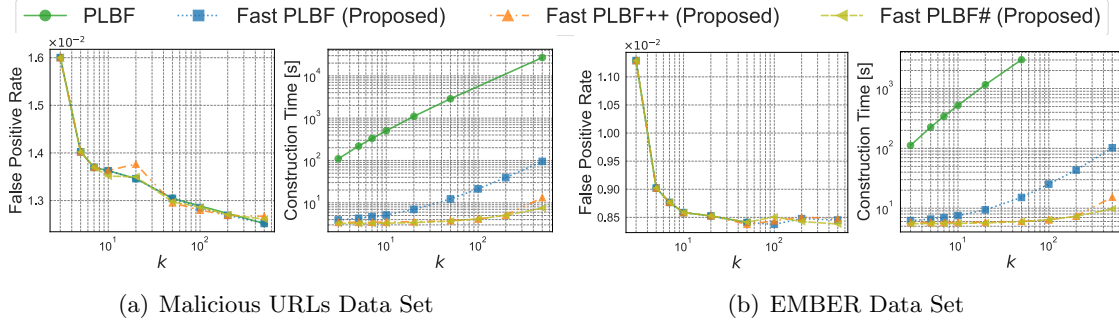
## 5.2 Memory Usage and FPR

We compared the trade-off between memory usage and FPR for the proposed methods with Bloom filter, Ada-BF, sandwiched LBF, and PLBF. Following the experiments in the original PLBF paper, hyperparameters for PLBFs were always set to  $N = 1,000$  and  $k = 5$ .

Figure 10 shows each method’s trade-off between memory usage and FPR. PLBF, fast PLBF, fast PLBF++, and fast PLBF# have better Pareto curves than the other methods for all data sets. Fast PLBF constructs the same data structure as PLBF in all cases, so it always has exactly the same accuracy as PLBF. In the hyperparameter settings here, fast PLBF++ and fast PLBF# also have the same data structure as PLBF in all cases and, therefore, have exactly the same accuracy as PLBF.

## 5.3 Ablation Study for Hyper-Parameters

The parameters of the PLBFs are total memory size,  $N$ , and  $k$ . The total memory size is specified by the user, and  $N$  and  $k$  are hyperparameters that are determined by balancing construction time and accuracy. In the previous sections, we set  $N$  to 1,000 and  $k$  to 5,

Figure 11: Ablation study for hyper-parameter  $N$ .Figure 12: Ablation study for hyper-parameter  $k$ .

following the original paper on PLBF. However, in this section, we perform ablation studies for these hyperparameters to confirm that our proposed methods can construct accurate data structures quickly, no matter what hyperparameter settings are used. We also confirm that the accuracy tends to be better and the construction time increases as  $N$  and  $k$  are increased, and that the proposed methods show a much slower increase in their construction time compared to PLBF.

Figure 11 shows the FPR and construction time with various  $N$  while the memory usage of the backup Bloom filters is fixed at 500 Kb and  $k$  is fixed at 5. For all four PLBFs, the FPR tends to decrease as  $N$  increases. Note that this is the FPR on test data, so it does not necessarily decrease monotonically. Also, as  $N$  increases, the PLBF construction time increases rapidly, but the fast PLBF construction time increases much more slowly than that, and for fast PLBF++ and fast PLBF#, the construction time changes little. This is because the construction time of PLBF is asymptotically proportional to  $N^3$ , while that of fast PLBF, fast PLBF++, and fast PLBF# is proportional to  $N^2$ ,  $N \log N$ , and  $N$ , respectively. The experimental results show that the three proposed methods can achieve high accuracy without significantly changing the construction time with large  $N$ .

Figure 12 shows the construction time and FPR with various  $k$  while the backup Bloom filter memory usage is fixed at 500 Kb and  $N$  is fixed at 1,000. For all four PLBFs, the FPR tends to decrease as  $k$  increases. For the EMBER data set, the FPR stops decreasing at about  $k = 20$ , while for the URLs data set, it continues to decrease even at about

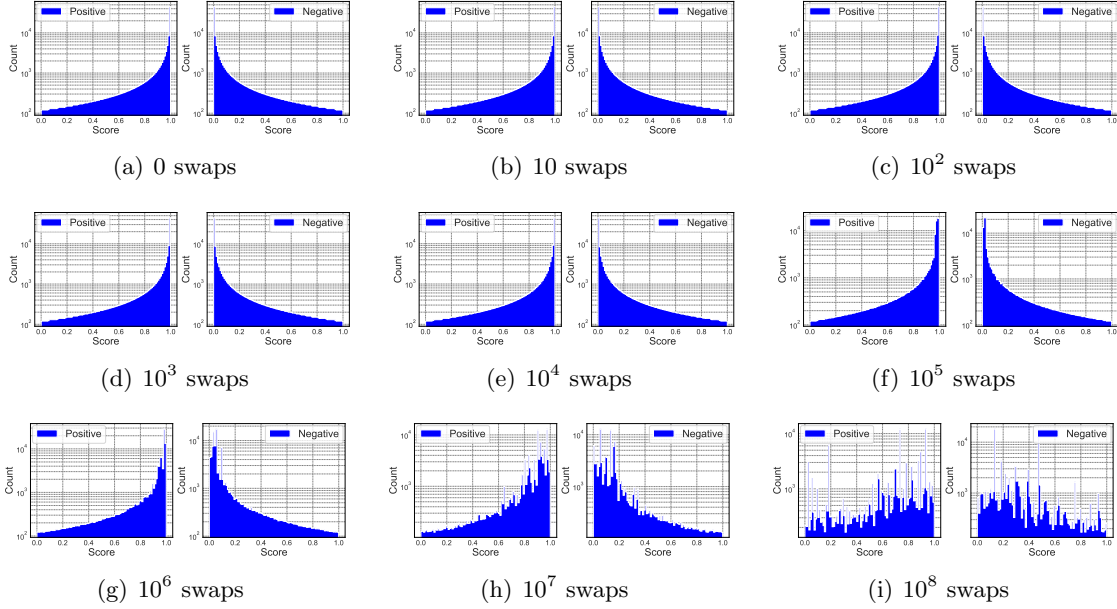


Figure 13: Score distribution histograms of artificial data sets (seed 0).

$k = 500$ . Just as in the case of experiments with varying  $N$ , this decrease is not necessarily monotonic because this is the FPR on test data. Fast PLBF always has the same accuracy as PLBF, but fast PLBF++ and fast PLBF# have slightly different accuracy from PLBF; fast PLBF++ exhibits up to 1.022 and 1.007 times the FPR of PLBF, and fast PLBF# exhibits up to 1.007 and 1.015 times FPR of PLBF for the URLs and EMBER data sets, respectively. In addition, the construction times of all four PLBFs increase proportionally to  $k$ , but fast PLBF has a much shorter construction time than PLBF, and fast PLBF++ and fast PLBF# have an even shorter construction time than fast PLBF. When  $k = 50$ , fast PLBF constructs 233 and 199 times faster, fast PLBF++ constructs 761 and 500 times faster, and fast PLBF# constructs 778 and 507 times faster than PLBF for the URLs and EMBER data sets, respectively. The experimental results indicate that by increasing  $k$ , the three proposed methods can achieve high accuracy without significantly affecting the construction time.

#### 5.4 Robustness of Fast PLBF++ and Fast PLBF# to Non-Ideal Distributions

Fast PLBF++ and fast PLBF# are not theoretically guaranteed to be as accurate as PLBF, except when the score distribution is *ideal*. Therefore, we evaluated the accuracy of fast PLBF++ by creating a variety of artificial data sets, ranging from data with monotonicity to data with little monotonicity. The results show that the smaller the monotonicity of the score distribution, the larger the difference in accuracy between fast PLBF++ and PLBF. We also observed that in most cases, the FPR for fast PLBF++ is within 1.1 times that of PLBF, but in cases where there is little monotonicity in the score distribution, the FPR of fast PLBF++ and fast PLBF# can be up to 1.85 times and 1.83 times that of PLBF, respectively.



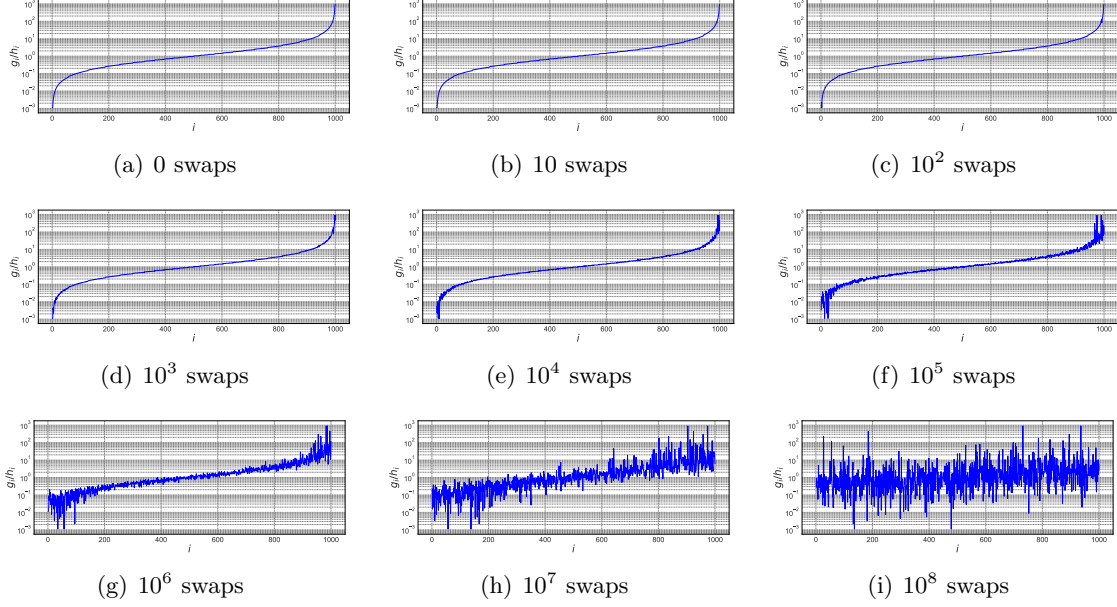


Figure 14: Ratio of key to non-key of artificial data sets (seed 0).

Here, we explain the process of creating an artificial data set, which consists of two steps. First, as in the original PLBF paper (Vaidya et al., 2021), the key and non-key score distribution is generated using the Zipfian distribution. Figure 13(a) shows a histogram of the distribution of key and non-key scores at this time, and Figure 14(a) shows  $g_i/h_i$  ( $i = 1, 2, \dots, N$ ) when  $N = 1,000$ . This score distribution is *ideal*. Next, we perform *swaps* to add non-monotonicity to the score distribution. *Swap* refers to changing the scores of the elements in the two adjacent segments so that the number of keys and non-keys in the two segments are swapped. Namely, an integer  $i$  is randomly selected from  $\{1, 2, \dots, N - 1\}$ , and the scores of elements in the  $i$ -th segment are changed so that they are included in the  $(i + 1)$ -th segment, and the scores of elements in the  $(i + 1)$ -th segment are changed to include them in the  $i$ -th segment. Figures 13(b) to 13(i) and Figures 14(b) to 14(i) show the histograms of the score distribution and  $g_i/h_i$  ( $i = 1, 2, \dots, N$ ) for  $10, 10^2, \dots, 10^8$  swaps, respectively. It can be seen that as the number of swaps increases, the score distribution becomes more non-monotonic. For each case of the number of swaps, 10 different data sets were created using 10 different seeds.

Figure 15 shows the accuracy of each method for each number of swaps, with the seed set to 0. Hyperparameters for PLBFs are set to  $N = 1,000$  and  $k = 5$ . It can be seen that fast PLBF and fast PLBF++ achieve better Pareto curves than the other methods for all data sets. It can also be seen that the higher the number of swaps, the more often there is a difference between the accuracy of fast PLBF++/# and fast PLBF.

Figure 16 shows the difference in accuracy between fast PLBF++/# and fast PLBF for each swap count. Here, the “relative false positive rate” is the false positive rate of fast PLBF++/# divided by that of PLBF constructed with the same hyperparameters and conditions. We created 10 different data sets for each swap count and conducted 6



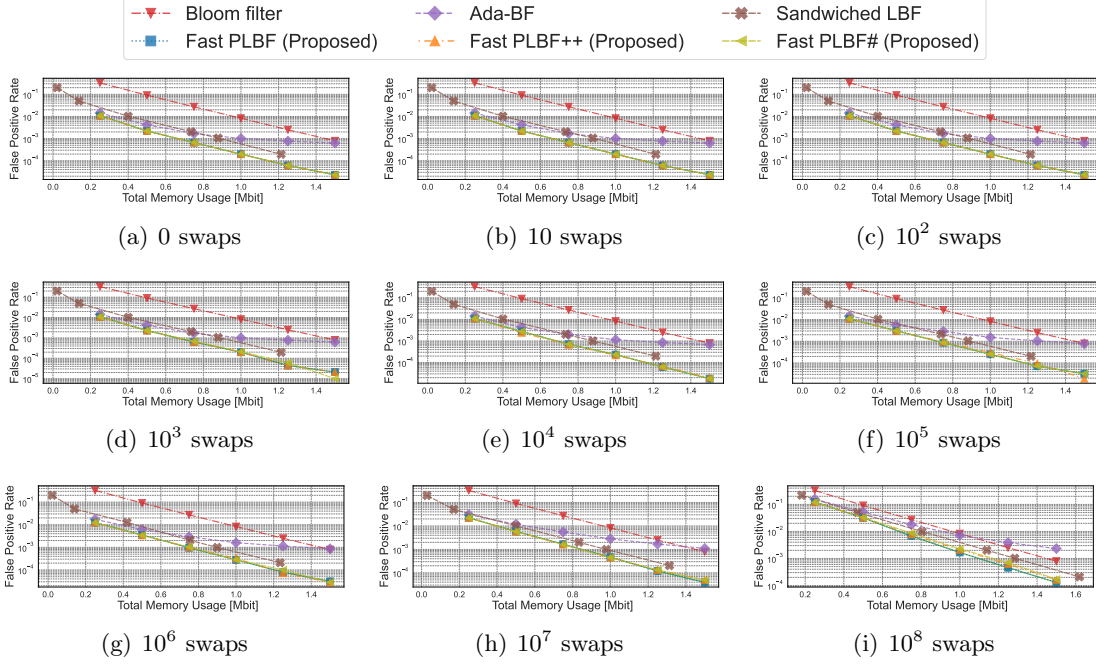


Figure 15: Trade-off between memory usage and FPR for artificial data sets (seed 0). The hyperparameters for PLBFs are  $N = 1,000$  and  $k = 5$ .

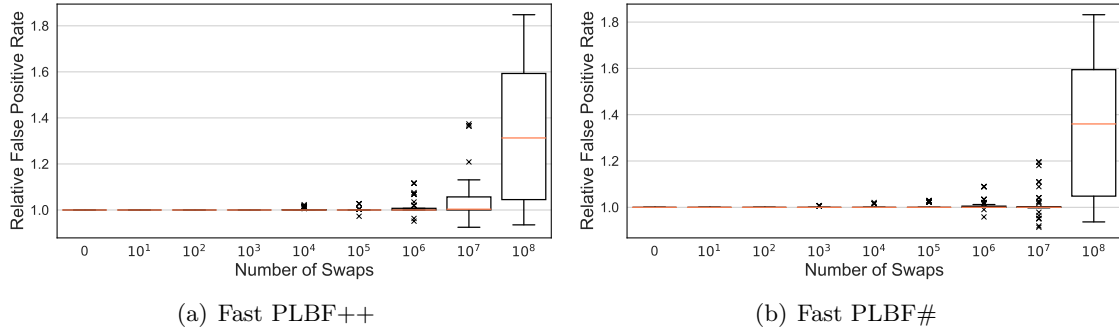


Figure 16: Distribution of the “relative false positive rate” of fast PLBF++ and fast PLBF# for each swap count. The “relative false positive rate” is the false positive rate of fast PLBF++ and fast PLBF# divided by that of PLBF constructed with the same hyperparameters and conditions.

experiments for each data set and method with a memory usage of 0.25Mb, 0.5Mb, 0.75Mb, 1.0Mb, 1.25Mb, and 1.5Mb. Namely, we compared the false positive rates of fast PLBF and fast PLBF++/# under 60 conditions for each swap count. The result shows that fast PLBF++ consistently achieves the same accuracy as PLBF in a total of 240 experiments where the number of swaps is  $10^3$  or less. Similarly, fast PLBF# consistently achieves the same accuracy as PLBF in a total of 180 experiments where the number of swaps is  $10^2$  or less. Furthermore, in the experiments where the number of swaps is  $10^7$  or less, the relative false positive rate is generally less than 1.1, with the exception of 14 cases for fast PLBF++ and 7 cases for fast PLBF#. However, in the cases of  $10^8$  swap counts, where there is almost no monotonicity in the score distribution, the false positive rate for fast PLBF++ and fast PLBF# is up to 1.85 times and 1.83 times that for PLBF, respectively.

## 6 Conclusion

PLBF is an outstanding LBF that can effectively leverage the distribution of the set and queries captured by a machine learning model. However, PLBF is computationally expensive to construct. We proposed fast PLBF and fast PLBF++ to solve this problem. Fast PLBF is superior to PLBF because fast PLBF constructs exactly the same data structure as PLBF but does so faster. Fast PLBF++ and fast PLBF# are even faster than fast PLBF and achieve almost the same accuracy as PLBF and fast PLBF. These proposed methods have greatly expanded the range of applications of PLBF.

## Acknowledgments and Disclosure of Funding

This work was supported by JST AIP Acceleration Research JPMJCR23U2, Japan. We appreciate the valuable feedback from the anonymous reviewers of NeurIPS, which has improved the quality of our paper and led to the development of new methods and analyses.

## References

- Alok Aggarwal, Maria M Klawe, Shlomo Moran, Peter Shor, and Robert Wilber. Geometric applications of a matrix-searching algorithm. *Algorithmica*, 2(1):195–208, 1987.
- Hyrum S Anderson and Phil Roth. Ember: An open dataset for training static pe malware machine learning models. *arXiv:1804.04637*, 2018.
- Burton H Bloom. Space/time trade-offs in hash coding with allowable errors. *Communications of the ACM*, 13(7):422–426, 1970.
- Andrei Broder and Michael Mitzenmacher. Network applications of bloom filters: A survey. *Internet Mathematics*, 1(4):485–509, 2004.
- Fay Chang, Jeffrey Dean, Sanjay Ghemawat, Wilson C Hsieh, Deborah A Wallach, Mike Burrows, Tushar Chandra, Andrew Fikes, and Robert E Gruber. Bigtable: A distributed storage system for structured data. *ACM Transactions on Computer Systems*, 26(2):1–26, 2008.
- Yifan Dai, Yien Xu, Aishwarya Ganesan, Ramnatthan Alagappan, Brian Kroth, Andrea Arpaci-Dusseau, and Remzi Arpaci-Dusseau. From wiskey to bourbon: A learned index for log-structured merge trees. In *USENIX Symposium on Operating Systems Design and Implementation (OSDI)*, 2020.
- Zhenwei Dai and Anshumali Shrivastava. Adaptive learned bloom filter (ada-bf): Efficient utilization of the classifier with application to real-time information filtering on the web. In *Advances in Neural Information Processing Systems (NeurIPS)*, 2020.
- Peter C. Dillinger and Stefan Walzer. Ribbon filter: Practically smaller than bloom and xor. *arXiv:2103.02515*, 2021.
- Jialin Ding, Umar Farooq Minhas, Jia Yu, Chi Wang, Jaeyoung Do, Yinan Li, Hantian Zhang, Badrish Chandramouli, Johannes Gehrke, Donald Kossmann, et al. Alex: An updatable adaptive learned index. In *ACM SIGMOD International Conference on Management of Data (SIGMOD)*, 2020.
- Bin Fan, Dave G Andersen, Michael Kaminsky, and Michael D Mitzenmacher. Cuckoo filter: Practically better than bloom. In *ACM International Conference on Emerging Networking Experiments and Technologies (CoNEXT)*, 2014.
- Paolo Ferragina and Giorgio Vinciguerra. The pgm-index: A fully-dynamic compressed learned index with provable worst-case bounds. In *International Conference on Very Large Data Bases (VLDB)*, 2020.

- Shahabeddin Geravand and Mahmood Ahmadi. Bloom filter applications in network security: A state-of-the-art survey. *Computer Networks*, 57(18):4047–4064, 2013.
- Michael T Goodrich and Michael Mitzenmacher. Invertible bloom lookup tables. In *Allerton Conference on Communication, Control, and Computing (Allerton)*, 2011.
- Thomas Mueller Graf and Daniel Lemire. Xor filters: Faster and smaller than bloom and cuckoo filters. *Journal of Experimental Algorithmics*, 25:1–16, 2020.
- Tu Gu, Kaiyu Feng, Gao Cong, Cheng Long, Zheng Wang, and Sheng Wang. The rlr-tree: a reinforcement learning based r-tree for spatial data. *Proceedings of the ACM on Management of Data*, 1(1):1–26, 2023.
- Chen-Yu Hsu, Piotr Indyk, Dina Katabi, and Ali Vakilian. Learning-based frequency estimation algorithms. In *International Conference on Learning Representations (ICLR)*, 2019.
- Johan Ludwig William Valdemar Jensen. Sur les fonctions convexes et les inégalités entre les valeurs moyennes. *Acta Mathematica*, 30(1):175–193, 1906.
- Guolin Ke, Qi Meng, Thomas Finley, Taifeng Wang, Wei Chen, Weidong Ma, Qiwei Ye, and Tie-Yan Liu. Lightgbm: A highly efficient gradient boosting decision tree. In *Advances in Neural Information Processing Systems (NeurIPS)*, 2017.
- Tim Kraska, Alex Beutel, Ed H Chi, Jeffrey Dean, and Neoklis Polyzotis. The case for learned index structures. In *ACM SIGMOD International Conference on Management of Data (SIGMOD)*, 2018.
- Pengfei Li, Hua Lu, Qian Zheng, Long Yang, and Gang Pan. Lisa: A learned index structure for spatial data. In *ACM SIGMOD International Conference on Management of Data (SIGMOD)*, 2020.
- Honghao Lin, Tian Luo, and David Woodruff. Learning augmented binary search trees. In *International Conference on Machine Learning (ICML)*, 2022.
- Guanlin Lu, Young Jin Nam, and David HC Du. Bloomstore: Bloom-filter based memory-efficient key-value store for indexing of data deduplication on flash. In *IEEE Symposium on Mass Storage Systems and Technologies (MSST)*, 2012.
- Michael Mitzenmacher. A model for learned bloom filters and optimizing by sandwiching. In *Advances in Neural Information Processing Systems (NeurIPS)*, 2018.
- Vikram Nathan, Jialin Ding, Mohammad Alizadeh, and Tim Kraska. Learning multi-dimensional indexes. In *ACM SIGMOD International Conference on Management of Data (SIGMOD)*, 2020.
- Anna Pagh, Rasmus Pagh, and S Srinivasa Rao. An optimal bloom filter replacement. In *ACM-SIAM Symposium on Discrete Algorithms (SODA)*, 2005.
- Atsuki Sato and Yusuke Matsui. Fast partitioned learned bloom filter. In *Advances in Neural Information Processing Systems (NeurIPS)*, 2023.

- Manu Siddhartha. Malicious urls dataset. <https://www.kaggle.com/datasets/sid321axn/malicious-urls-dataset>, 2021. [Online; accessed 22-December-2022].
- Sasu Tarkoma, Christian Esteve Rothenberg, and Eemil Lagerspetz. Theory and practice of bloom filters for distributed systems. *IEEE Communications Surveys & Tutorials*, 14(1):131–155, 2011.
- Kapil Vaidya, Eric Knorr, Michael Mitzenmacher, and Tim Kraska. Partitioned learned bloom filters. In *International Conference on Learning Representations (ICLR)*, 2021.
- Minmei Wang and Mingxun Zhou. Vacuum filters: More space-efficient and faster replacement for bloom and cuckoo filters. In *International Conference on Very Large Data Bases (VLDB)*, 2019.
- Meifan Zhang, Hongzhi Wang, Jianzhong Li, and Hong Gao. Learned sketches for frequency estimation. *Information Sciences*, 507:365–385, 2020.
- Zhou Zhang, Zhaole Chu, Peiquan Jin, Yongping Luo, Xike Xie, Shouhong Wan, Yun Luo, Xufei Wu, Peng Zou, Chunyang Zheng, et al. Plin: A persistent learned index for non-volatile memory with high performance and instant recovery. In *International Conference on Very Large Data Bases (VLDB)*, 2022.

## Appendix A. Solution of the Optimization Problems

In the original PLBF paper (Vaidya et al., 2021), the analysis with mathematical expressions was conducted only for the relaxed problem, while no analysis utilizing mathematical expressions was performed for the general problem. Consequently, it was unclear which calculations were redundant, leading to the repetition of constructing similar DP tables. Hence, this appendix provides a comprehensive analysis of the general problem. It presents the optimal solution and the corresponding value of the objective function using mathematical expressions. This analysis uncovers redundant calculations, enabling the derivation of fast PLBF.

The optimization problem designed by PLBF (Vaidya et al., 2021) can be written as follows:

$$\begin{aligned}
& \underset{\mathbf{f}, \mathbf{t}}{\text{minimize}} && \sum_{i=1}^k c|\mathcal{S}|G_i \log_2 \left( \frac{1}{f_i} \right) \\
& \text{subject to} && \sum_{i=1}^k H_i f_i \leq F \\
& && t_0 = 0 < t_1 < t_2 < \dots < t_k = 1 \\
& && f_i \leq 1 \quad (i = 1, 2, \dots, k).
\end{aligned} \tag{57}$$

The objective function represents the total memory usage of the backup Bloom filters. The first constraint equation represents the condition that the expected overall FPR is below  $F$ .  $c \geq 1$  is a constant determined by the type of backup Bloom filters.  $\mathbf{G}$  and  $\mathbf{H}$  are determined by  $\mathbf{t}$ . Once  $\mathbf{t}$  is fixed, we can solve this optimization problem to find the optimal  $\mathbf{f}$  and the minimum value of the objective function. In the original PLBF paper (Vaidya et al., 2021), the condition  $f_i \leq 1$  ( $i = 1, 2, \dots, k$ ) was relaxed; however, here we conduct the analysis without relaxation.

First, in the case of  $\sum_{i \in \{j | G_j > 0\}} H_i \leq F$ , the minimum value of the objective function is clearly 0. This is because if we set

$$f_i = \begin{cases} 0 & (G_i = 0) \\ 1 & (G_i > 0), \end{cases} \tag{58}$$

the conditions of the optimization problem are satisfied, and the value of the objective function (which is always non-negative) becomes 0. In addition, even assuming that  $H_i = 0 \Rightarrow f_i = 1$ , it has no effect on the solution to the optimization problem. This is because even if there is an  $i$  that satisfies  $H_i = 0 \wedge f_i < 1$ , the  $\mathbf{f}$  that can be obtained by changing  $f_i$  to 1 satisfies the conditions of the optimization problem and has the same or a smaller value for the objective function. Therefore, in the following, we will consider the case of  $\sum_{i \in \{j | G_j > 0\}} H_i > F$ , and assume that  $H_i = 0 \Rightarrow f_i = 1$ .

The Lagrange function is defined using the Lagrange multipliers  $\boldsymbol{\mu} \in \mathbb{R}^k$  and  $\nu \in \mathbb{R}$ , as follows:

$$L(\mathbf{f}, \boldsymbol{\mu}, \nu) = \sum_{i=1}^k c|\mathcal{S}|G_i \log_2 \left( \frac{1}{f_i} \right) + \sum_{i=1}^k \mu_i (f_i - 1) + \nu \left( \sum_{i=1}^k H_i f_i - F \right). \tag{59}$$

From the KKT condition, there exist  $\bar{\mu}$  and  $\bar{\nu}$  in the local optimal solution  $\bar{\mathbf{f}}$  of this optimization problem, and the following holds:

$$\frac{\partial L}{\partial f_i}(\bar{\mathbf{f}}, \bar{\mu}, \bar{\nu}) = 0 \quad (i = 1, 2, \dots, k) \quad (60)$$

$$\bar{f}_i - 1 \leq 0, \quad \bar{\mu}_i \geq 0, \quad \bar{\mu}_i(\bar{f}_i - 1) = 0 \quad (i = 1, 2, \dots, k) \quad (61)$$

$$\sum_{i=1}^k H_i \bar{f}_i - F \leq 0, \quad \bar{\nu} \geq 0, \quad \bar{\nu} \left( \sum_{i=1}^k H_i \bar{f}_i - F \right) = 0. \quad (62)$$

By introducing  $\mathcal{I}_{f=1} = \{i | \bar{f}_i = 1\}$ , Equations (60) to (62) can be organized as follows:

$$c|\mathcal{S}|G_i = \bar{\mu}_i + \bar{\nu}H_i, \quad \bar{\mu}_i \geq 0, \quad \bar{f}_i = 1 \quad (i \in \mathcal{I}_{f=1}), \quad (63)$$

$$c|\mathcal{S}|G_i = \bar{f}_i \bar{\nu} H_i, \quad \bar{\mu}_i = 0, \quad \bar{f}_i < 1 \quad (i \notin \mathcal{I}_{f=1}), \quad (64)$$

$$\sum_{i \in \mathcal{I}_{f=1}} H_i + \sum_{i \notin \mathcal{I}_{f=1}} H_i \bar{f}_i - F \leq 0, \quad \bar{\nu} \geq 0, \quad \bar{\nu} \left( \sum_{i \in \mathcal{I}_{f=1}} H_i + \sum_{i \notin \mathcal{I}_{f=1}} H_i \bar{f}_i - F \right) = 0. \quad (65)$$

Here, we can prove  $\bar{\nu} > 0$  by contradiction. Assuming  $\bar{\nu} = 0$ , Equation (64) implies that  $\bar{f}_i < 1 \Rightarrow G_i = 0$ ; that is,  $G_i > 0 \Rightarrow \bar{f}_i = 1$ . However, this does not satisfy the conditions of the optimization problem, as  $\sum_{i=1}^k H_i \bar{f}_i \geq \sum_{i \in \{j | G_j > 0\}} H_i \bar{f}_i = \sum_{i \in \{j | G_j > 0\}} H_i > F$ . Therefore, we have  $\bar{\nu} > 0$ .

Noting that we are assuming  $H_i = 0 \Rightarrow f_i = 1$ , we obtain the following from equations  $\bar{\nu} > 0$  and Equation (64):

$$\bar{f}_i = \frac{c|\mathcal{S}|}{\bar{\nu}} \frac{G_i}{H_i} \quad (i \notin \mathcal{I}_{f=1}). \quad (66)$$

From Equations (65) and (66) and  $\bar{\nu} > 0$ , we obtain

$$\frac{c|\mathcal{S}|}{\bar{\nu}} = \frac{F - \sum_{i \in \mathcal{I}_{f=1}} H_i}{1 - \sum_{i \in \mathcal{I}_{f=1}} G_i}, \quad (67)$$

where  $G_{f=1}$  and  $H_{f=1}$  are defined in Equation (5). Thus, we get

$$\bar{f}_i = \begin{cases} 1 & (i \in \mathcal{I}_{f=1}) \\ \frac{(F - H_{f=1})G_i}{(1 - G_{f=1})H_i} & (i \notin \mathcal{I}_{f=1}). \end{cases} \quad (68)$$

Substituting this into the objective function of the optimization problem (Equation 3), we obtain

$$\sum_{i=1}^k c|\mathcal{S}|G_i \log_2 \left( \frac{1}{\bar{f}_i} \right) = \sum_{i \notin \mathcal{I}_{f=1}} -c|\mathcal{S}|G_i \log_2 \left( \frac{F - \sum_{j \in \mathcal{I}_{f=1}} H_j G_j}{1 - \sum_{j \in \mathcal{I}_{f=1}} G_j} \frac{G_i}{H_i} \right) \quad (69)$$

$$= c|\mathcal{S}|(1 - G_{f=1}) \log_2 \left( \frac{1 - G_{f=1}}{F - H_{f=1}} \right) - c|\mathcal{S}| \sum_{i \notin \mathcal{I}_{f=1}} G_i \log_2 \left( \frac{G_i}{H_i} \right). \quad (70)$$

We can also obtain the conditions of  $\mathcal{I}_{f=1}$ . First, from the assumption,

$$H_i = 0 \Rightarrow i \in \mathcal{I}_{f=1}. \quad (71)$$

Using  $\bar{\nu} > 0, c > 0, |\mathcal{S}| > 0$ , Equation (63) and Equation (67) derives

$$i \in \mathcal{I}_{f=1} \wedge H_i > 0 \Rightarrow \frac{G_i}{H_i} \geq \frac{\bar{\nu}}{c|\mathcal{S}|} = \frac{1 - G_{f=1}}{F - H_{f=1}}, \quad (72)$$

and Equation (64) and Equation (67) derives

$$i \notin \mathcal{I}_{f=1} \Rightarrow \frac{G_i}{H_i} < \frac{\bar{\nu}}{c|\mathcal{S}|} = \frac{1 - G_{f=1}}{F - H_{f=1}}. \quad (73)$$

## Appendix B. Modification of the PLBF Framework

In this appendix, we describe the framework modifications we made to PLBF in our experiments. In the original PLBF paper (Vaidya et al., 2021), the optimization problem was designed to minimize the amount of memory usage under a given target FPR (Equation 3). However, this framework makes it difficult to compare the results of different methods and hyperparameters. Therefore, we designed the following optimization problem, which minimizes the expected FPR under a given memory usage condition:

$$\begin{aligned} & \underset{\mathbf{f}, \mathbf{t}}{\text{minimize}} && \sum_{i=1}^k H_i f_i \\ & \text{subject to} && \sum_{i=1}^k c|\mathcal{S}| G_i \log_2 \left( \frac{1}{f_i} \right) \leq M \\ & && t_0 = 0 < t_1 < t_2 < \dots < t_k = 1 \\ & && f_i \leq 1 \quad (i = 1, 2, \dots, k), \end{aligned} \quad (74)$$

where  $M$  is a parameter that is set by the user to determine the upper bound of memory usage.

Introducing  $\mathcal{I}_{f=1}$  for analysis as we have done in Appendix A, it follows that the optimal FPRs  $\bar{\mathbf{f}}$  is

$$\bar{f}_i = \begin{cases} 1 & (i \in \mathcal{I}_{f=1}) \\ 2^{-\beta} \frac{G_i}{H_i} & (i \notin \mathcal{I}_{f=1}) \end{cases}, \quad (75)$$

where

$$\beta = \frac{M}{c|\mathcal{S}|(1 - G_{f=1})} + \frac{1}{1 - G_{f=1}} \sum_{i \notin \mathcal{I}_{f=1}} G_i \log_2 \left( \frac{G_i}{H_i} \right). \quad (76)$$

When  $\mathbf{f} = \bar{\mathbf{f}}$ , the expected FPR, that is, the objective function of Equation (74) is

$$H_{f=1} + 2^{-\beta}(1 - G_{f=1}). \quad (77)$$

Therefore, as in the original framework, we can find the best  $\mathbf{t}$  and  $\mathbf{f}$  by finding a way to cluster the 1st to  $(j-1)$ -th segments into  $k-1$  regions that maximizes  $\sum_{i=1}^{k-1} G_i \log_2 (G_i/H_i)$  for each  $j = k, k+1, \dots, N$ . We can find it using the same DP algorithm and its acceleration methods as in the original framework.